CCMT

Center for Compressible Multiphase Turbulence

Microscale Experiments

PI: Don Littrell
AFRL Munitions Directorate
Eglin AFB, FL

- Goals
  - Few, miniature-sized particles
  - Well-known explosive
  - Extract V&V data for simulation models
- Test Setup
  - 2mm dia. Tungsten particles
  - 9g N-5 with RP-83 detonator
  - 2" dia. mild steel casing
  - Pencil probes, infrared cameras, high speed video, x-rays

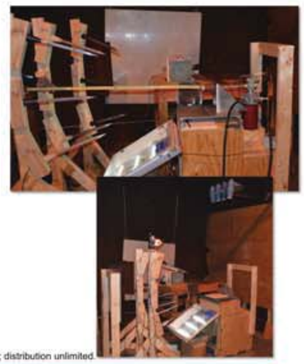

First Round – October 2014

- Single particle

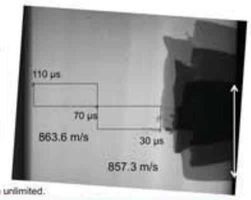

First Round – October 2014

- Ring of 7 particles

- Grid of 16 particles

Second Round – February 2015

- Improvements:
  - 8 pressure probes, mounted as a grid
  - 4 x-ray images
  - Improved camera settings
- Test Sequence
  - 6 gas-valve tests
  - 6 explosively driven tests
  - Configurations
    - Single tungsten sphere
    - 3 tungsten hexes
    - Salt
    - 4 tungsten spheres, diamond pattern

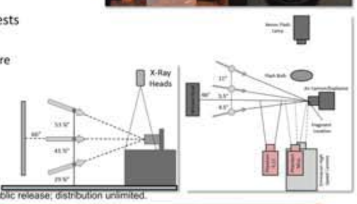

Second Round – February 2015

Test #	Test Description
#07	Rp83 + 3 N5 + Single Small Tungsten Sphere
#08	Rp83 + 3 N5 + Single Small Tungsten Sphere
#09	Rp83 + 3 N5 + 3 Tungsten Hexes
#10	Rp83 + 3 N5 + Salt
#11	Rp83 + 3 N5 + Salt
#12	Rp83 + 3 N5 + 4 Diamond Pattern of Small Tungsten Spheres

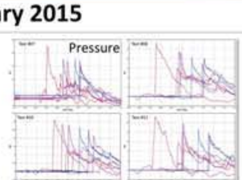

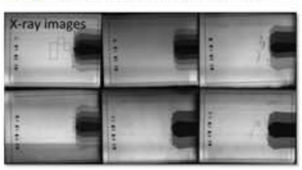

High speed Phantom Miro 310

High speed Phantom 6.11

High speed SIMACON

Key Results and Future Work

- 2 rounds of microscale testing complete
- Enhanced diagnostics from Round 2 from lessons learned
- Gas field measurements from pressure probes and high speed videos
- Particle location and velocity from x-ray images

- UF analysis of experimental data
  - Simulations
  - Uncertainty Quantification
- Round 3 of testing to address lessons learned from UF analysis

UF UNIVERSITY of FLORIDA · NNSA

CCMT

Center for Compressible Multiphase Turbulence

Mesoscale Experiments

PI: C. Mike Jenkins
AFRL Munitions Directorate
Eglin AFB, FL

- Goals
  - $>10^3$ particles, 100-120 μm sieved particles
  - Well-known explosive
  - Extract V&V data for simulation models
- Test Setup
  - Compressed gas and explosive tests
  - 112μm Tungsten powder
  - 3-6g N-5 with RP-80 detonator
  - 4" dia. hardened steel casing
  - Pencil probes, infrared cameras, high speed video, x-rays

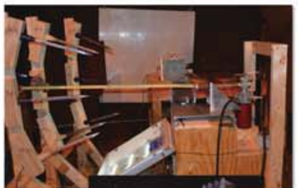


Dynamic Test Environment

- Compressed gas tests
  - Shots 1-12
  - Coarse steel powder (1-7) and Tungsten powder (8-12)
  - X-ray timing
  - Camera resolution / framing rate / light delay
- Explosive tests
  - Shots 13-22
  - 0.5g Tungsten powder pressed in tissue
  - Further refinement of x-ray timing
  - Further refinement of camera settings



X-ray images

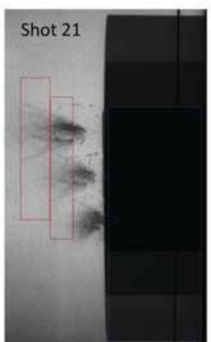

Pressure Data

- Probes measure time of arrival of the blast wave

Probe	Location (in)
1	32
2	31.25
3	31.875
4	31.75
5	31.25
6	31.875
7	32.25
8	32
9	31.375

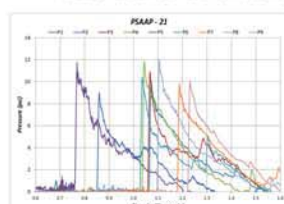


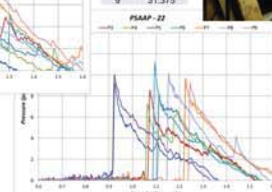

High Speed Video (Representative)

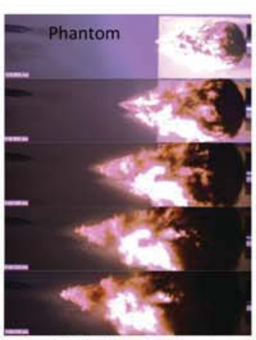

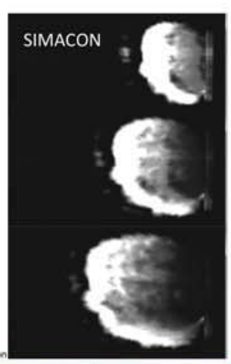

Key Results and Future Work

- Round 1 of mesoscale testing complete
- Enhanced diagnostics from Microscale lessons learned
- Gas field measurements from pressure probes and high speed videos
- Particle location and velocity from x-ray images

- UF analysis of experimental data
  - Simulations
  - Uncertainty Quantification
- Round 2 of testing
  - Address lessons learned from UF analysis
  - Gas gun tests – no fireball
  - Particle Image Velocimetry (PIV)


UF UNIVERSITY of FLORIDA

NNSA

CCMT

Center for Compressible Multiphase Turbulence

In-situ External Calibration

Student: Heather Zunino
Advisor: Prof. Ronald Adrian
Department: MAE, ASU

- Goals
  - Develop a method for calibrating cameras which can be performed entirely outside the measurement region
- Simulation roadmap
  - The experiments performed at Arizona State University use a closed test section—a shock tube. This proposed method will simplify and potentially improve the camera calibration required for these experiments.

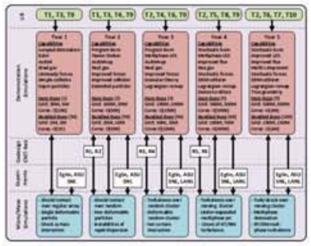

Simulation Roadmap

Motivation

- Correct for image distortion using camera calibration

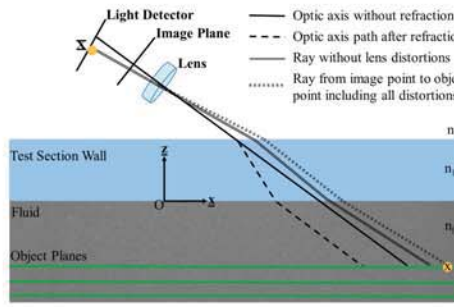

Results

	Position of Camera	Location of Calibration Plate
Standard (II)	*in-situ*	Internal
Option (EE)	*ex-situ*	External
Proposed (IE)	*in-situ*	External

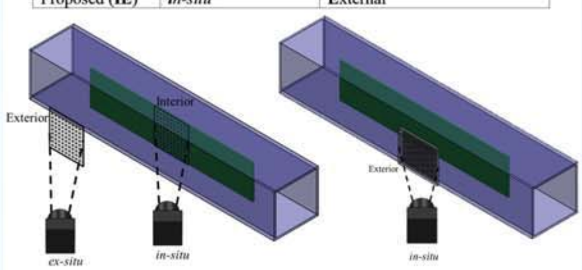

Results

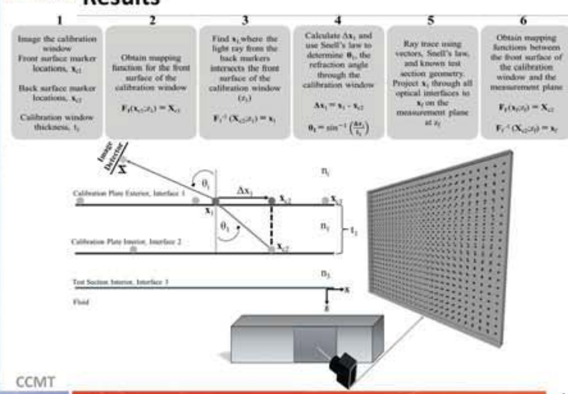

Results

- The *in-situ* exterior (IE) calibration experiment yielded results only slightly worse than the *in-situ* internal (II) method
- The IE method measured displacements to ± 0.014mm (averaged over the entire measurement plane)
  - This translates to slightly larger than one pixel
- For comparison, the II method was able to measure to ± 0.005mm
  - This translates to approximately one half pixel
- The greater error of the IE method is attributed to the use of out-of-focus images of the calibration plate
  - It is more difficult to locate the center of out-of-focus images, because they are spread out over more pixels. In this case, the diameters of the images used for IE calibration were four times larger than the images used for II calibration.

Summary

- *In-situ* external calibration is useful for experiments where the experimenter cannot insert and remove the calibration target from the test section without moving the cameras or other optical components.
- Additionally, the experimenter may want to employ the IE method if relative motion is expected to occur between the imaging system and the flow during experimental realizations (e.g. shock tubes and other experiments with energetic flows), as this may be accounted for if the calibration window remains installed during the experiment.
  - In this scenario, the calibration markers would be used as spatial fiducial markers in each image.

References

- Adrian, R.J. and Westerweel, J. 2010 *Particle Image Velocimetry*. Cambridge University Press
- Solo, M.D. and Adrian, R.J. 1997 *Distortion compensation for generalized stereoscopic particle image velocimetry*. Measurement Science and Technology **8** 1441-1454.
- Wieneke, B. 2008 *Volume self-calibration for 3D particle image velocimetry*. Experiments in Fluids **45** 549-556
- Wieneke B 2004 *Application of self-calibration stereo PIV in enclosed measurement volumes*. 12th international symposium on the application of laser techniques to fluid mechanics Lisbon, Portugal.

CCMT

Center for Compressible Multiphase Turbulence

Uncertainty Budget for CMT Simulation

Dr. Chanyoung Park
Department: CCMT, UF

- Goals
  - V&V and UQ
  - Planning experiments and model developments for efficient uncertainty reduction
  - UQ tool developments
  - Interaction for applying creative techniques
- Simulation roadmap
  - T3: JWL-EOS based on surrogate model
  - T4: Validation, UQ and UR of the shock tube simulation

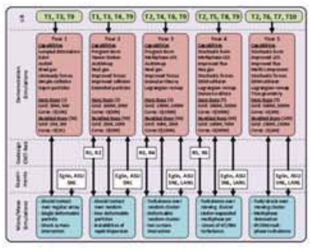

Simulation Roadmap

CCMT 1

Multi-Fidelity Surrogate Modeling

- Tackling challenge of UQ for computationally intensive simulations
  - MFSs can emulate meso/macroscale 3D simulations based on combined samples from 1D/2D/3D simulations
- Extrapolation of scarce high fidelity data with aid of sufficient low fidelity data
  - The performance of CMT-nek can be estimated by combining performance data from CMT-nek and CMT-bone-BE

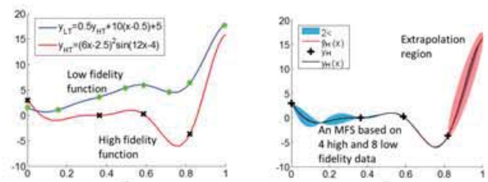

CCMT 2

Cost Saving vs. Accuracy Improvement

Total budget		0.25	0.1	0.033
56H	Max cost saving	50%	75%	83%
	Max RMSE reduction	23%	48%	49%
28H	Max cost saving	58%	75%	88%
	Max RMSE reduction	11%	22%	37%

- Various MFS frameworks examined with Hartmann6 function for different computational budgets (28H and 56H) and cost ratios (0.25, 0.1 and 0.033)
- MFS was mostly useful for saving computational cost rather than improving accuracy
- Calibration based MFS frameworks performed consistently well with a few high fidelity samples
- Saving computational cost makes computationally intensive UQ of the macro simulations affordable

CCMT 3

The Role of Regression Scalar

- Discrepancy function has been widely used to calibrate low fidelity surrogates to high fidelity responses $\hat{y}_H(\mathbf{x}) = \rho \hat{y}_L(\mathbf{x}) + \hat{\delta}(\mathbf{x})$
- Accuracy of the discrepancy surrogate is the key to accurate MFS
- Finding ρ and fitting a discrepancy function together was found to be beneficial by simplifying discrepancy

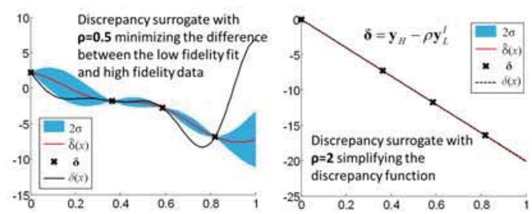

CCMT 4

Extrapolation Aspect of MFSs

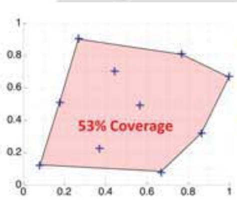

- MFS prediction is usually extrapolation in terms of high-fidelity data
- The tendency intensifies as dimension increases with few high fidelity samples
- Studying reliable extrapolation strategy using various MFS frameworks

Total budget	Best RMSE	RMSE of the extrapolation domain	RMSE of the interpolation domain	Coverage of extrapolation domain (%)
56H	0.130	0.133	0.086	92%
28H	0.166	0.167	0.103	96.5%

CCMT 5

Extrapolation for CMT-nek

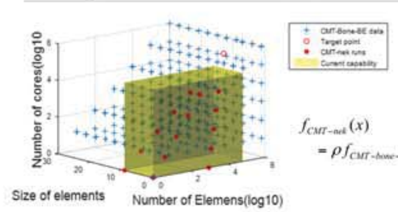

$$f_{CMT-nek}(x) = \rho f_{CMT-bone-BE}(x) + f_{disc}(x)$$

- The UB team and the exascale team are planning prediction (extrapolation) of the execution time of CMT-nek using MFS
- MFS will extrapolate (predict) the execution time of CMT-nek based on execution time samples from CMT-bone-BE
- The discrepancy function calibrates CMT-bone-BE to CMT-nek
- Typical large error in extrapolation is expected to be mitigated using MFS

CCMT 6

UF UNIVERSITY of FLORIDA · NNSA

CCMT

Center for Compressible Multiphase Turbulence

Convergence in Simulations

Student: Maria Giselle Fernandez-Godino

Collaborator: Dr. Angela Diggs

Advisors: Drs. Haftka & Balachandar

Department: MAE, UF

- Goals
  - Verification of 1D simulations
- Simulation roadmap
  - Mesoscale simulations of the shock curtain interaction.

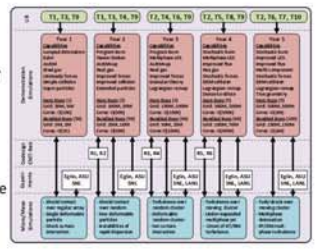

Simulation Roadmap

CCMT 1

Lack of Convergence in 1D simulations

- The goal of any numerical simulation is to accurately capture chosen physical observations

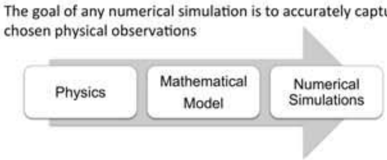

- Lax's theorem: Consistency +Stability = Convergence
- We believe based on previous experience that our scheme (RK3 + AUSM+up) is consistent
-
  - Due to numerical instability (i.e., violation of CFL condition)
  - Due to instability of mathematical model

CCMT 2

Shock –Curtain Interaction: Grid dependence

- Ever increasing instability with increasing grid discretization

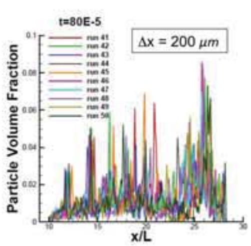

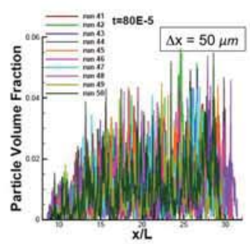

PVF as a function of x/L (L=initial particle curtain thickness) at t=80e-5 s for 10 random initial particles distributions.

CCMT 3

Run-to-Run Variation in the Mean

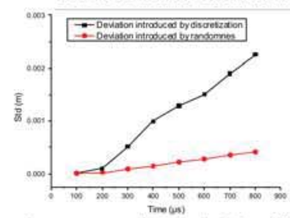

(Black) Standard deviation (Std) of the mean curtain location as a function of time for changes in the grid size. (Red) Standard deviation of the mean curtain particles mean as a function of time for changes in the initial particle distribution.

- No convergence due to intrinsic instability that increases with wavenumber
- An instability theory has been developed for analysis
- Inter-particle collisional force slows the instability, but does not stabilize
- Particle Based (PB) method to calculate PVF removes oscillation, but does not yield complete convergence (see next slide)
- Proposed Solution: Diffusion due to gas-mediated interaction

CCMT 4

Particle Based (PB) Volume Fraction

- PB volume fraction calculation results in a smoother profile, however the PVF variation due to the grid change is still higher than the one introduced by the random initial position cases.

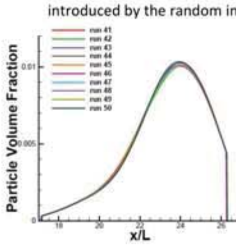

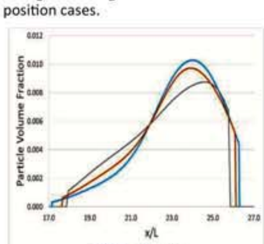

PVF as a function of x/L. Left figure shows PVF for 10 random initial position of particles cases. Right figure shows PVF for 50, 100 and 250 μm grid sizes.

CCMT 5

Summary

- Convergence = Consistency + Stability
- We believe that our scheme is consistent
- The non-convergence behavior is due to volume fraction dependent drag induced small-scale instability
- Inter-particle collisional force is not sufficient to stabilize the instability
- A simple theory has been developed to investigate the instability
- Particle-Based volume fraction calculation reduces oscillation and improves convergence
- A diffusion term is needed in the particle volume fraction equation to capture gas-mediated particle-particle interaction.

CCMT 6

UF UNIVERSITY of FLORIDA

NNSA

CCMT

Center for Compressible Multiphase Turbulence

Review of Shock Tube Experiments

Student: Justin Mathew
Advisor: Prof. Kim and Prof. Haftka
Department: MAE, UF

- Goals
  - Reproduce results and understand methodologies of existing shock tube studies
  - Identify metrics and results that can be used to validate simulation code
- Simulation roadmap
  - T2: Multiphase turbulence modeling and uncertainty
  - T4: Validation, UQ and UR of the shock tube simulation

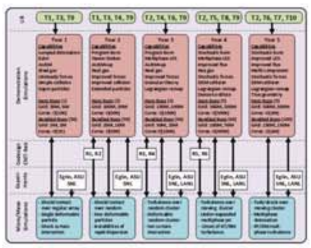

Simulation Roadmap

Motivation

- The study of shock tube experiments presents an opportunity to identify parameters that can be used to validate computational simulation code
- Two experiments have predominately been studied
  - Studies of vertical shock tube experiments at ASU conducted by Heather Zunino have been studied to determine and characterize input and output parameters that would be used to validate turbulence model developed by the simulation team.
  - Horizontal shock tube experiments conducted by Justin Wagner at Sandia National Labs are studied to identify and understand uncertainty sources in the experiments
  - Most recently Dr. Wagner's particle curtain experiments have been studied in order to understand and characterize the methodology used to measure volume fraction as determined by x-ray images of the shock and particle curtain interaction
  - These characterizations are used to validate the shock tube code to simulate the particle curtain and shock interaction in the horizontal shock tube.

Uncertainty in Vertical Shock Tubes

- Reviews of vertical shock tube experiments conducted at ASU were focused on identifying sources of uncertainty that should be quantified
- In these experiments, a particle bed is subjected to rapid decompression as a diaphragm is ruptured between a vacuum-like pressure region and a particle bed at atmospheric pressure
- Bed height is a metric to be used for simulation data validation
  - Identification and definition of bed height remains to be studied further
- Of particular interest from an uncertainty perspective are the following aspects of the experiment:
  - Bed packing – initial volume fraction of particle bed
  - Effect of the diaphragm
    - Before rupture, an initial deflection of the diaphragm is observed due to pressure
    - After rupture, the diaphragms behavior is not entirely consistent
  - Reflected shock and expansion fan and their associated effects

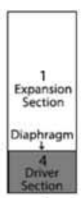

Using X-ray Images to Obtain Volume Fraction

- Using x-ray images provided by Dr. Wagner, the methodology to determine the volume fraction of a particle curtain in a horizontal shock tube is studied and results from Dr. Wagner's experiments are reproduced
- The volume fraction profiles for five time points are determined and plotted. Each profile is an average of four images

Raw image at $t=0$

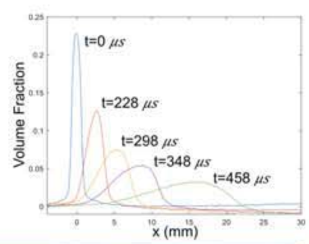

Curtain Thickness and Front Locations

- Curtain thickness and front locations are more easily and accurately measured using Schlieren images
- A methodology to determine and validate measurements of curtain thickness and front locations using X-ray images is of particular interest
- These front locations are currently identified by where the volume fraction is 5% of the maximum
- To establish some metric of consistency the profile is integrated between the upstream and downstream front locations to yield a measurement of volume

Time Delay (μs)	Curtain Thickness (mm)	Measurement of Volume	Upstream Location (mm)	Downstream Location (mm)
0	3.1	0.3244	-1.5	1.6
228	5.7	0.3433	-0.7	5
298	10.7	0.3751	-1.9	8.8
348	12.8	0.3665	-0.2	12.6
458	22.4	0.3754	-0.3	22.1

Year 3 Goals

- Efforts in the future will be directed towards further understanding methodologies used to identify front locations for both horizontal and vertical shock tube experiments
- Validation criterion are to be developed using front locations determined by Schlieren images compared to those found by X-ray
- Confirmed methods will be used to supply metrics and results by which computational code developed to simulate particle curtain and shock interactions can be validated
- Uncertainty from volume fraction estimates from X-ray images will also be quantified using existing and adapted methods

UF UNIVERSITY of FLORIDA

CCMT

Center for Compressible Multiphase Turbulence

Force Model Sensitivity Analysis in 1-D Shock-Particle Interaction

Student: Sam Nili
Collaborator: Dr. Chanyoung Park
Advisor: Prof. Kim & Haftka
Department: MAE, UF

- Goals
  - Quantify the effect of errors in force terms to evaluate their contribution
  - Done with sensitivity analysis
- Simulation roadmap
  - T4: Verification and validation of the shock tube simulation

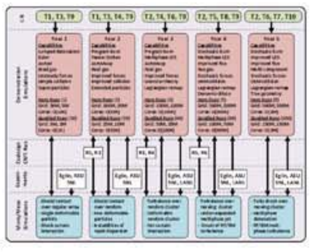

Simulation Roadmap

Motivation

- Due to large length scale of the computational domain compared to the particle sizes for the shock tube simulation approximate models are often used to investigate the shock-particle interaction.
- Force on particle (P) is sum of five components, all approximate: quasi-steady (QS), pressure gradient (PG), added mass (AM), viscous unsteady (VU) and inter-particle interaction (IP) force.

$$f^P = f_{qs} + f_{pg} + f_{am} + f_{uv} + f_{ip}$$

- In order to find which approximate models should be improved, uncertainty quantification of these numerical models is crucial.

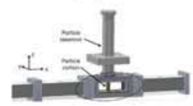

Schematic of the multiphase shock tube test section

Photograph of the particle curtain acquired with a test section, wall removed

Local Sensitivity of Front Particle Location on Forces

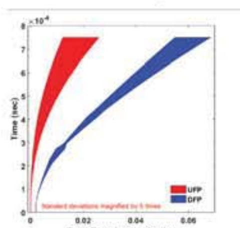

Effect of 10% error perturbation in quasi-steady force on front particle location

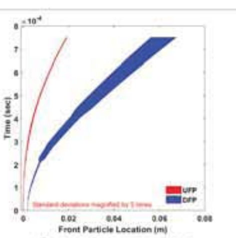

Effect of 10% error perturbation in added mass force on front particle location

Effect of 10% error perturbation in individual force terms on standard deviation(SD) of FP location at t = 750 μs

	QS	PG	AM	VU	IP
UFP SD (m)	0.0007	0.00001	0.00001	0.000002	0.00003
DFP SD (m)	0.0007	0.0003	0.0005	0.00003	0.0003

Global Force Uncertainty Contribution on UFP Location

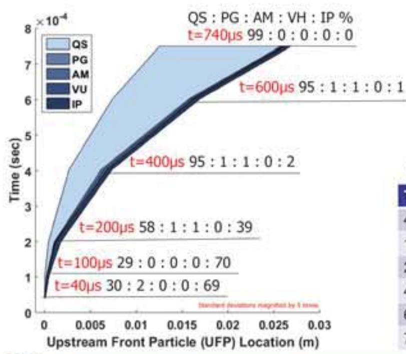

Sensitivity Parameter

$$S_{Z_i} = \frac{V(E(Y|Z_i))}{V(Y)}$$

Total Standard Deviation

Time (μs)	SD (μm)
40	2.52
100	15.8
200	67.7
400	348
600	672
750	920

Global Force Uncertainty Contribution on DFP Location

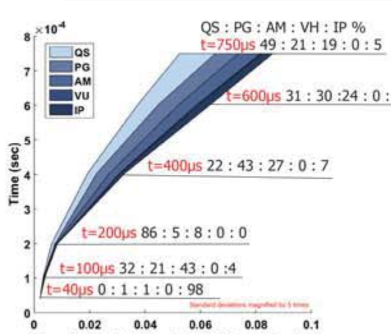

t=750μs Uncertainty Contribution

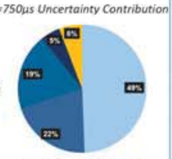

Time (μs)	SD (μm)
40	2.48
100	15.3
200	42.7
400	178
600	418
750	665

Summary

- The errors is randomly generated utilizing Latin Hypercube Sampling (LHS) and perturbed into the forces within +-10% bounds, both locally and globally.
- The contribution of each error in forces on front particle movement is investigated by measuring its influence on standard deviation of front particle location.
- Local sensitivity study shows that possible errors in the quasi-steady and added mass forces are dominant for for downstream front position (DFP).
- Global sensitivity study shows that quasi-steady force is dominant for model uncertainty for upstream front particle (UFP).
- For UFP, The effect of Inter-particle interaction force decreases as the shock develops.
- For the DFP, dominant forces change as the shock moves.
- The effect of the inter-particle interaction is dominant at the early stage for DFP.
- More than 94 % of Error in DFP is a first order effect (no interaction).
- More than 99 % of Error in UFP is a first order effect.

UF UNIVERSITY of FLORIDA

CCMT

Center for Compressible Multiphase Turbulence

Uncertainty Reduction Using Extrapolation

Student: Yiming Zhang
Advisor: Prof. Kim and Prof. Haftka
Department: MAE, UF

- Goals
  - Develop extrapolation methods to estimate discretization error of shock simulation (Microscale)
  - Build multi-fidelity model of behavioral emulation for UR
- Simulation roadmap
  - T4: Verification and validation of the shock tube simulation
  - Exascale: Emulate computation performance of exascale architectures for early algorithm design space exploration

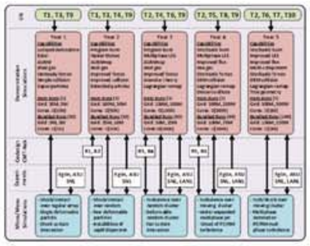

Simulation Roadmap

Motivation and Progress

- Extrapolate discretization error of microscale shock simulation
  - Challenges: (1) Convergence study with unstructured tetrahedral elements and multiple grid parameters (3) Mixed order of convergence (p=1~2)
  - Progress: Tested various methods regarding oscillatory convergence especially when Richardson Extrapolation fails (e.g. p<0.5 or p>2)
- Enhance performance prediction of behavioral simulation using multi-fidelity surrogate
  - Motivation: Prediction error of behavioral emulation may be corrected using statistical model calibration
  - Progress: Evaluated current theoretical tools using test functions

Microscale Shock Simulation

- There are five particles in each of the planes 1, 3 and 5, and four particles in each of the planes 2 and 4
- A shock is initialized upstream of the particles at t=0 and travels downstream in the x-direction.
- Peak drag coefficient C_D of center particles on plane 1,3,5 are quantity of interest

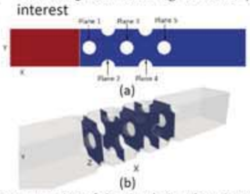

(a) x-y cut-section of the simulation domain at z = 0
(b) isometric view of the simulation domain showing distribution of particles in the y − z planes.

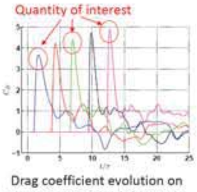

Drag coefficient evolution on planes 1 to 5 from left to right

$$\tau = \frac{\text{shock speed}}{\text{radius of particle}}$$

Mesh Refinement of Shock Simulation

- Candidate error estimators from Eça, L., & Hoekstra, M. (2014)
  - Four alternative estimators: selection by least standard deviation

$$\delta_{RE} = \phi_i - \phi_0 = \alpha h_i^p \qquad \delta_1 = \phi_i - \phi_0 = \alpha h_i$$
$$\delta_2 = \phi_i - \phi_0 = \alpha h_i^2 \qquad \delta_{12} = \phi_i - \phi_0 = \alpha_1 h_i + \alpha_2 h_i^2$$

  - Estimated error U_ϕ: Discretization error $\varepsilon_\phi(\phi_i)$+ overall noise level σ+ difference with extrapolation curve

$$\phi_i - U_\phi \le \phi_{exact} \le \phi_i + U_\phi \qquad |\phi_i - \phi_{fit}|. \quad F_s = 1.25$$
$$U_\phi(\phi_i) = F_s \varepsilon_\phi(\phi_i) + \sigma + |\phi_i - \phi_{fit}|$$

  - Secondary factors were fixed: relative size of domain and surface element, time step, shock thickness, Mach number
  - Monitored representative size of all the FEA elements in spatial space to check deformation of unstructured element through refinement (Effort from Microscale team)

Discretization Error of Shock Simulation

- Candidate error estimators from Eça, L., & Hoekstra, M. (2014)
  - Four sets of grids with refinement ratio of 1.1
  - Representative element size based on regular tetrahedron

$$h_d = (6\sqrt{2}V/N)^{1/3}$$

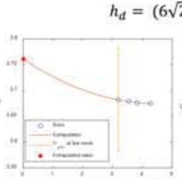

(a) Plane 1: Estimator δ_{12} U_ϕ at fine mesh is 2.7%

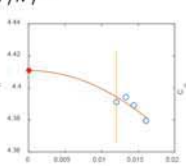

(b) Plane 3: Estimator δ_2 U_ϕ at fine mesh is 0.6%

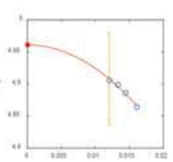

(c) Plane 5: Estimator δ_2 U_ϕ at fine mesh is 1.5%

Behavioral Emulation and Extrapolation

- Prediction error of behavioral emulation is expected to be compensated by a scale factor ρ and discrepancy function $f_{discrepancy}(x)$

$$f_{CMTbone-BE}(x) = \rho f_{Behavioral\ emulation}(x) + f_{discrepancy}(x)$$

- Examined various methods to estimate ρ and $f_{discrepancy}(x)$

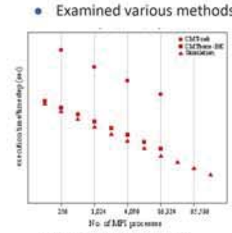

Fig.4. Conceptual Graphs

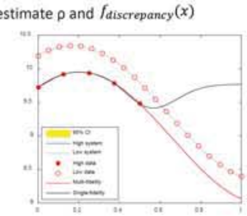

Fig.5. Illustration of multi-fidelity model using test function



CCMT

Center for Compressible Multiphase Turbulence

CMT-nek Development & Transition

Dr. Jason F. Hackl

Department: MAE, UF

- Goals
  - Development of CMT-nek
  - Scalable high-resolution compressible flow solver
  - Variational, discontinuous Galerkin (DG) treatment of multiphase source terms
- Simulation roadmap
  - T9: weak-form DG framework for conservation laws & high-order operators on tensor-nested spectral elements
  - Inviscid interaction between spheres and ASU expansion

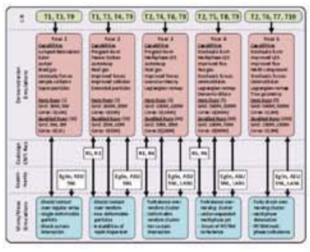

Simulation Roadmap

CMT-nek: Path to Prediction at Exascale

- Explosive dispersal: Compressible Multiphase Turbulence
  - Coupled complex flow physics
  - Tremendous range of scales (μm → m, μs → ms)
  - Shock waves interact with unresolved flows around point particles; models affect small-scale solution regularity

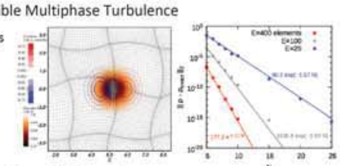

- Discontinuous Galerkin extends Spectral Element Method of nek5000 toward robust stabilization of irregularity, yet efficient and scalable resolution of compressible turbulent flow phenomena
- Adapting shock capturing techniques to high-order polynomial representation is still open to research
- Implementation challenges in nek5000 also exist

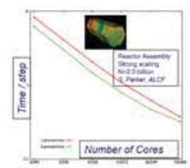

CMT-nek: governing equations

$$\mathbf{U} \equiv \phi_g \begin{bmatrix} \rho \\ \rho u \\ \rho v \\ \rho w \\ \rho E \end{bmatrix} \rightarrow \frac{\partial U_i}{\partial t} + \nabla \cdot \mathbf{H}_i(\mathbf{U}, \nabla \mathbf{U}) = R_i$$

flux = convective + diffusive

$$\mathbf{H}_i = \mathbf{H}_i^c(\mathbf{U}) + \mathbf{H}_i^d(\mathbf{U}, \nabla \mathbf{U})$$

Mass

$$\mathbf{H}_i^c = \phi_g \begin{bmatrix} \rho u \\ \rho v \\ \rho w \end{bmatrix}, \mathbf{H}_1^d = 0$$

Momentum

$$\mathbf{H}_2^c = \phi_g \begin{bmatrix} (\rho u)u + p \\ (\rho u)v \\ (\rho u)w \end{bmatrix}, \mathbf{H}_3^c = \phi_g \begin{bmatrix} (\rho u)u \\ (\rho u)v + p \\ (\rho u)w \end{bmatrix}, \mathbf{H}_4^c = \phi_g \begin{bmatrix} (\rho u)u \\ (\rho u)v \\ (\rho u)w + p \end{bmatrix}$$

$$H_{i+1,j}^d = -\phi_g \tau_{ij} \quad H_{ij}^d = G_{ijkl} \frac{\partial U_k}{\partial x_l}$$ Viscous flux Jacobian

Energy

$$\mathbf{H}_5^c = \phi_g(\rho E + p) \begin{bmatrix} u \\ v \\ w \end{bmatrix}, H_{5j}^d = -\phi_g(u_k \tau_{kj} + q_j)$$

Gas-particle coupling

$$\mathbf{R} = -\begin{bmatrix} \mathcal{C}_{gp} \\ p \nabla \phi_g + \mathcal{M}_{gp} \\ p u_j (\partial \phi_g / \partial x_j) + \mathcal{E}_{gp} \end{bmatrix}$$

CMT-nek: Discontinuous Galerkin (DG)

Flux divergence

$$\mathbf{U} \equiv \phi_g \begin{bmatrix} \rho \\ \rho u \\ \rho v \\ \rho w \\ \rho E \end{bmatrix} \rightarrow \frac{\partial U_i}{\partial t} + \nabla \cdot \mathbf{H}_i(\mathbf{U}, \nabla \mathbf{U}) = R_i$$

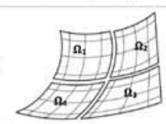

- nek5000 traditionally keeps advection in "strong form"
  - But DG's variational inner product with test function *v* needs integration by parts **twice**
  - Introduces **two** surface fluxes across faces (otherwise discontinuous)

$$\int_{\Omega_e} v \frac{\partial U}{\partial t} dV = \int_{\partial \Omega_e} v(\mathbf{H} - \mathbf{H}^*) \cdot \mathbf{n} \, dA - \int_{\Omega_e} v(\nabla \cdot \mathbf{H}) \, dV + \int_{\Omega_e} vR \, dV$$

- CMT-nek applies spectral element operators to "weak form"
  - Integration by parts **once** is more robust for discontinuous Galerkin methods.

$$\int_{\Omega_e} v \frac{\partial U}{\partial t} dV = \int_{\Omega_e} (\nabla v) \cdot \mathbf{H} \, dV - \int_{\partial \Omega_e} v \mathbf{H}^* \cdot \mathbf{n} \, dA + \int_{\Omega_e} vR \, dV$$

Results Concurrent with Development

- CMT-nek is already used for inviscid forces on spheres in expansion fans

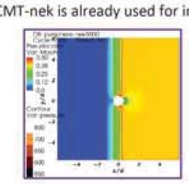

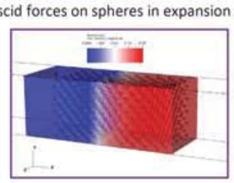

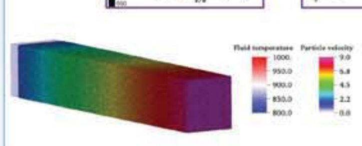

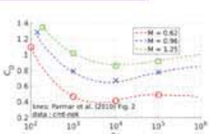

- Particle tracking algorithm admits nonlinear particle force models

Y3: Weak Form of Higher-Order Operators

- Weak form conserves mass much better than strong form
  - Variational crime still prevents lifting
  - Future migration from Gauss-Legendre-Lobatto to Gauss-Legendre points will enable tensor nesting *without* variational crime

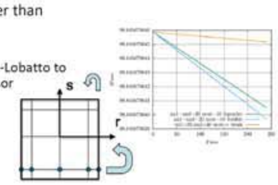

- Strong form **unsuited** to DG of viscous terms
- Starting on weak form for higher-order operators

$$\int_{\Omega_e} v \mathbf{S} \, dV = -\int_{\Omega_e} (\nabla v) U \, dV + \int_{\partial \Omega_e} v U^* \mathbf{n} \, dA$$

$$H_j^d = \mathbb{A}_{j,ik} \left[\frac{\partial U_i}{\partial x_k} \right] = \int_{\Omega_e} (\nabla v) \cdot \mathbf{S} \, dV - \int_{\partial \Omega_e} v \mathbf{S}^* \cdot \mathbf{n} \, dA$$

UF UNIVERSITY of FLORIDA

NNSA

CCMT

Center for Compressible Multiphase Turbulence

CMT-nek Particle Capabilities

Student: David Zwick
Advisor: Dr. S. Balachandar
Department: MAE, UF

- Goals
  - Rigorously understand link between Eulerian-Lagrangian/ Eulerian-Eulerian multiphase simulations
  - Particle modeling
  - CMT-nek code development
- Simulation roadmap
  - Detailed modeling of particle simulations in ASU experiment in CMT-nek
  - 1-way coupling

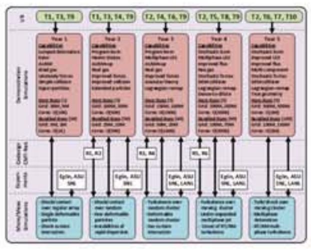

Simulation Roadmap

Motivation

- Force modeling of particles in compressible flow
- Comparing with ASU experiment

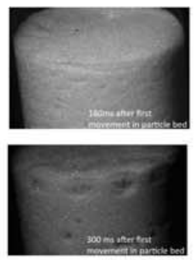

ASU Experiment

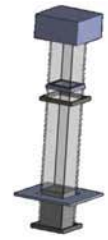

ASU setup

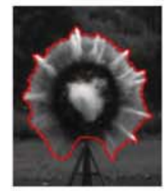

Frost experiment

Particle Timing Improvements

- "New" CMT-nek code improvements compared to "old" nek5000 SVN code
- Times are in ms per CPU per timestep

Particles	125,000		1,000,000		3,375,000	
	Old	New	Old	New	Old	New
Flow solver	32.37	32.08	32.41	32.24	32.57	32.48
Particle tracking time	45.54	21.46	207.91	34.82	641.29	77.58
Get computational coordinates	39.36	18.93	173.17	20.27	533.40	28.06
Send to destination MPI rank	-	0.30	-	1.83	-	7.71
Interpolation	5.17	1.49	33.49	11.85	105.57	39.97

Lagrangian Physics in CMT-nek

- Governing equation of particle motion (1-way coupled)

$$m_p \frac{\partial \vec{v}}{\partial t} = \vec{F}_{qs} + \vec{F}_{un} + \vec{F}_{iu}$$

- Quasi-steady force

$$\vec{F}_{qs} = S(\vec{u} - \vec{v}) C_D \qquad S = \frac{Re_p m_p}{24\tau_p}$$

- Undisturbed force

$$\vec{F}_{un} = m_g \frac{D\vec{u}}{Dt}$$

- Inviscid unsteady force

$$\vec{F}_{iu} = \frac{1}{2} V_p \left(\rho_g \frac{D\vec{u}}{Dt} - \frac{\partial \rho_g \vec{v}}{\partial t} \right) C_M$$

Finite Mach and Reynolds number corrections:
$C_D(Re_p, M_p)$
$C_M(M_p)$

Force History

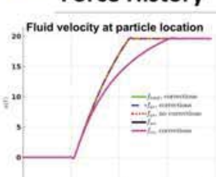

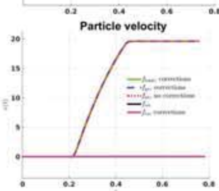

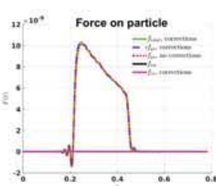

- Expansion fan sweeping over a single particle
- Fan begins at x = 0.5 and moves left
- Particle initially at rest at x = -8.0
- Pressure ratio across rarefaction is ~2.0
- Stokes number is 0.01

Year 3 Goals

- Goals for Year 3
  - 2-way coupling
    - Rigorous implementation that preserves higher-order accuracy
  - Force modeling
    - Currently CMT-nek has basic force modeling, but models are not the final answer for compressible physics
    - Microscale models developed at the Center will be fed into macroscale simulation
  - Comparison with ASU experiment

UF UNIVERSITY of FLORIDA   NNSA

CCMT

Center for Compressible Multiphase Turbulence

CMT-nek Microscale Simulation

Student: Goran Marjanovic

Advisor: Dr. S. Balachandar

Department: MAE, UF

- Goals
  - Demonstrate CMT-nek capabilities
  - Verification
  - Validation
- Simulation roadmap
  - Microscale simulation
    - Expansion over curtains of particles

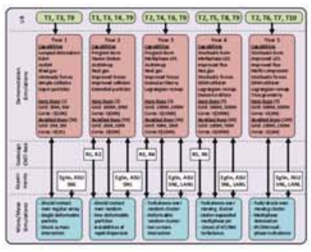

Simulation Roadmap

Motivation

- Validation of ASU experiments with the current CMT-nek physics capabilities
- Verification using current theory for expansion fan over particles

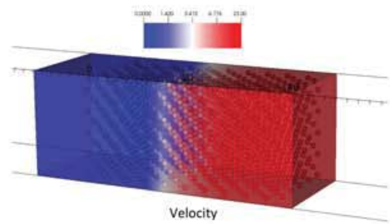

Velocity

Expansion Fan Over Particles

- Face centered cubic array of 1,000 spheres of unit diameter
  - 20 layers of 50 particles each
- 134x20x20 domain
- 69,200 elements with a polynomial order of 9
- High resolution spheres
  - 24 elements per sphere
  - 17,496 grid points per sphere
- 50,446,800 degrees of freedom

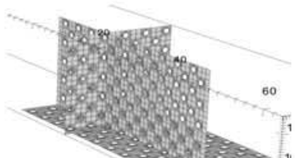

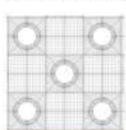

Results Using CMT-nek

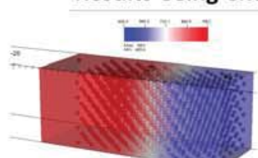

Pressure

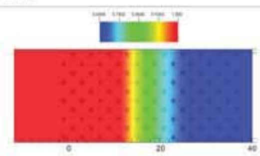

Density

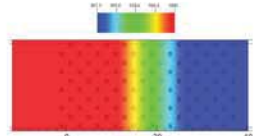

Temperature

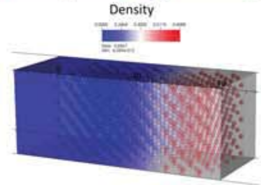

Mach Number

Drag Histories of Different Particle Layers

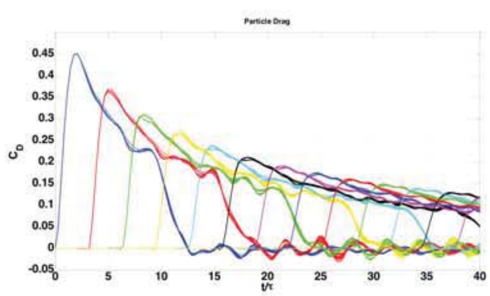

Year 3 Goals

- Extend microscale runs to upcoming CMT-nek code
  - Navier-Stokes solver
  - Shock capturing capabilities
- Validate using Justin Wagner's shock tube particle curtain experiments
- Verify analytical results of shock waves over particles

UF UNIVERSITY of FLORIDA

NNSA

CCMT

Center for Compressible Multiphase Turbulence

Mesoscale Particle Rarefaction in CMT-nek

Student: Bradford Durant
Advisor: Dr. S. Balachandar
Department: MAE, UF

- Goals
  - Demonstrate particle capability in CMT-nek
  - Simulate Mesoscale physics in CMT-nek
  - Validate meso physics with ASU experimentation data
- Simulation roadmap
  - Year 2 calls for improved forces and collision on particles. This simulation is fulfilling the mesoscale side of this role.

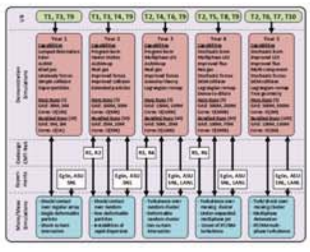

Simulation Roadmap

Motivation

- Mesoscale effects will occur and must be captured in the simulation of the demonstration problem to ensure sufficient accuracy

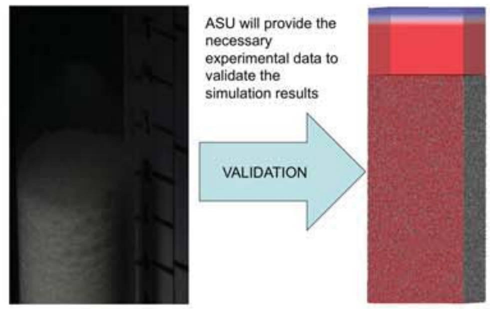

Rarefaction Passing Through Particle Bed

- **Current Simulation**
  - 1 Million point Grid
  - 8 Million Particles
  - Pressure Ratio 2.17
- **Forces Simulated**
  - Quasi-steady
  - Added Mass
  - Mach number corrections
  - Re number corrections
  - Undisturbed Force

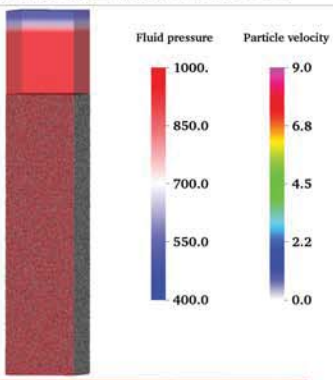

Results: Side View

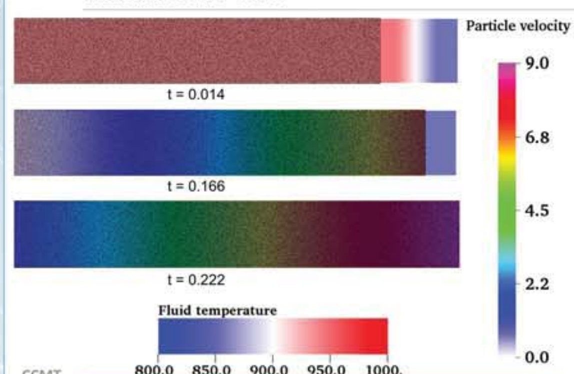

Results: Isometric View

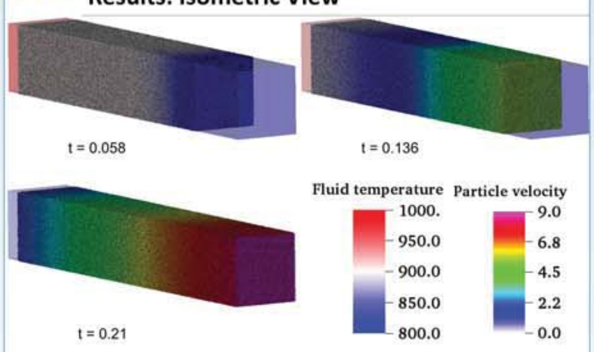

Year 3 Goals

- Improve the Mesoscale Simulation
  - Increase particle and grid count
  - Add volume fraction effects to particle forces
  - Include end of tube effects
  - Include family of runs with varying pressure ratios

CCMT

Center for Compressible Multiphase Turbulence

Surrogate Modeling of Equation of State

Student: Frederick Ouellet
Advisor: Dr. S. Balachandar
Department: MAE, UF

- Goals
  - Develop a surrogate model for use in evaluating the equation of state in mixed air/product cells
  - Analyze the effects of perturbations in initial conditions on the demonstration problem
- Simulation roadmap
  - Real gas equation of state capabilities in code
  - Analysis of instabilities of rapid dispersion

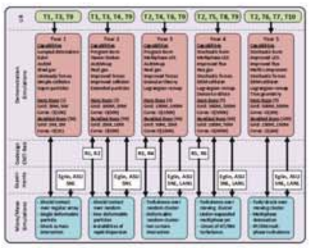

Simulation Roadmap

Motivation

Equation of State	Initial PETN Detonation Temperature (K)
Ideal Gas	7944.25
JWL	4501.40
Experimental Result	4140

- Real gas equations of state are needed for explosive products
- Iterative methods for handling mixed product-air cells are computationally expensive
- A surrogate model would provide a faster alternative

Explosive dispersal of a packed bed of sand particles

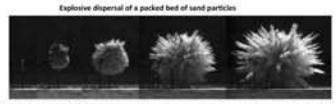

(D. L. Frost, Y. Gregoire, O. Petel, S. Goroshin, and F. Zhang, "Particle jet formation during explosive dispersal of solid particles," Physics of Fluids, vol. 24, no. 9, p. 1109, 2012.)

- The pictures taken by Frost et al. during their detonation experiments show the formation of coherent jets at late time. We believe that initial detonation conditions and/or particle distribution may play a role in their formation.

Surrogate Model - Development

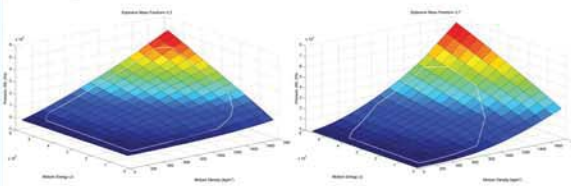

Slices of surrogate model for pressure at explosive mass fractions of 0.3 (left) and 0.7 (right)
White boundary represents the convex hull of the model

- Kriging method used to generate surrogate model for pressure and temperature in mixed cells in terms of mixture density, energy and explosive mass fraction
- Model replaces iterative Broyden's Method solver with matrix multiplication
- Not all combinations of mixture quantities generate physically possible values of pressure/temperature → beginning of convex hull idea

Surrogate Model – Preliminary Results

Simulation Description

- 2D, Quarter-Cylinder grid
  - Outer radius = 0.3 m
    - 150,000 cells
      - Gas-Only

- Preliminary runs with the surrogate model show minimal differences in the blast wave radius compared to the iterative method
- Since these runs are only gas, no particle effects have been analyzed as of now
- Looking into effective methods to reduce this difference

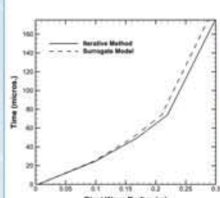

Run	Time Steps/s (Iterative JWL)	Time Steps/s (Surrogate)	% Difference
1	7.389	18.956	156.54
2	7.273	19.865	173.13
3	7.325	19.057	160.16
Avg.	7.329	19.292	163.23

Effects of Initial Conditions

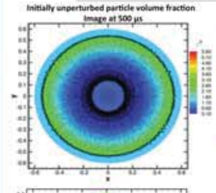

- Introduction of perturbations in initial particle volume fraction lead to "jetting" in the particle and gas fields
- We took azimuthal bi-modal perturbations of the form

$$\phi^p = \phi_0^p[1 + Acos(k_1\theta) + Acos(k_2\theta)]$$

- The size of the resulting structures are amplified if the mode numbers are in-phase compared to out-of-phase
- This follows the results by Wei and Livescu [1] for two-fluid RT instabilities

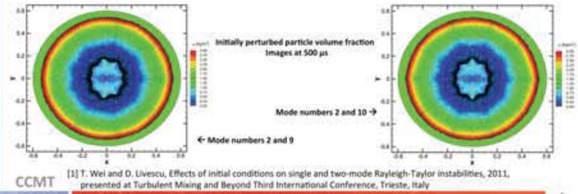

[1] T. Wei and D. Livescu, Effects of initial conditions on single and two-mode Rayleigh-Taylor instabilities, 2011, presented at Turbulent Mixing and Beyond Third International Conference, Trieste, Italy

Summary & Year 3 Goals

- Summary
  - Developed a surrogate model to handle real gas calculations in mixed air-product cells
  - Surrogate model shows minimal differences in the location of the blast wave compared to the iterative method
  - Surrogate model speeds up the code when used instead of the iterative method
  - Analyzed effect of bi-modal initial perturbations in the particle volume fraction around the explosive, found that if the two mode numbers of the perturbation are in phase, the growth of the resulting structures in the particle and gas fields is amplified compared to out of phase mode numbers
- Year 3 Goals
  - Develop a method to have the convex hull of the surrogate allow simulations to sense when they are reaching the boundary of physically allowable variable values and manage appropriately
  - Work on improved particle collision and compaction models for more accurate and realistic simulations at higher particle volume fractions. This work will focus on finding better possible alternatives to the currently used Harris-Crighton model.

CCMT

Center for Compressible Multiphase Turbulence

Particle-Based Volume Fraction Calculation

Dr. Angela Diggs
AFRL, Eglin AFB, FL

- Goals
  - High-fidelity Eulerian-Lagrangian (EL) coupling
  - EL AUSM+up
  - Validation against Sandia multiphase experiments
- Simulation roadmap
  - Rigorous error-estimation of EL implementation (T9)
  - Critical evaluation of inter-particle collision model (T4) and volume fraction effects (T6)

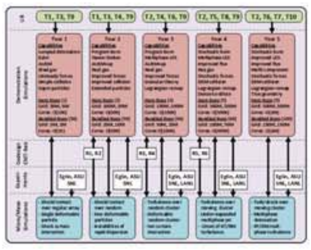

Simulation Roadmap

Motivation

- Shock Induced Particle Flow

- Simulation Setup
  - 1d shock tube
  - 100 µm particles
  - Mesoscale validation against Sandia experiments
  - Address all the fundamental challenges in Eulerian-Lagrangian simulations of particle-particle interaction dominated flows

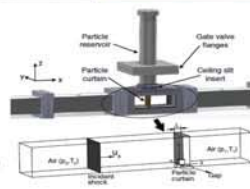

E-L Coupling: Volume Fraction

- Grid-based methods:
  - Linear projection (Ling et al, 2012)
  - Sum particles in grid cell (Balakrishnan et al., 2010)
- Particle curtain in uniform flow, $F_{qs}(\alpha_p) \sim F_{qs}\frac{1+2\alpha_p}{(1-\alpha_p)^2}$
  - Expect: translation downstream
  - Conventional Eulerian methods:
    - Widening upstream curtain
    - Wild downstream oscillations
- Particle-based method:

$$\alpha_{Gauss,j} = \frac{1}{S}\sum_{i=1}^{N_{cp}}\frac{1}{\delta\sqrt{\pi}}exp\left[-\delta(X_j - X_i)^2\right]$$

  - Maintains sharp edges
  - Allows sub-grid resolution

Gaussian PB method reduces numerical error in volume fraction calculation.

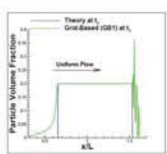

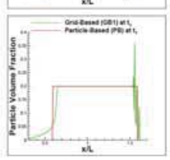

Von Neumann Error Analysis

- von Neumann analysis: total error and components
  - Deterministic error = discretization error + bias error
    - Discretization error caused by using a finite number of grid cells
    - Bias error caused by using a finite number of computational particles
- Grid-based (GB)
  - Zeroth order: particles contribute to the Eulerian grid cell where they reside
  - First order: particles contribute linearly to two cells
  - Second order (discrete delta): particle contributes to three cells
- Particle-based (PB)
  - Top-hat: equal weight to all particles within δ of the reference particle
  - Gaussian: Gaussian weight given to particles within δ of the reference particle

Moderate sinusoidal

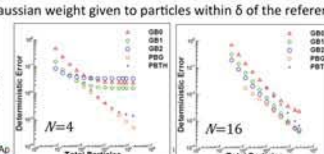

Flux Schemes For Multiphase Flows

- AUSM+up flux scheme
  - Multiphase Eulerian-Eulerian developed by Liou et al. (2008)
  - Single phase AUSM (1993), AUSM+ (1996), AUSM+up (2006)
- Extension to Eulerian-Lagrangian
  - Balanced pressure flux terms

$$f_{k,j+\frac{1}{2}} = \frac{1}{2}\left(\dot{m}_{k,j+\frac{1}{2}} + \left|\dot{m}_{k,j+\frac{1}{2}}\right|\right)\begin{Bmatrix}\alpha\\ \alpha u\\ \alpha H\end{Bmatrix}_{k,L} + \frac{1}{2}\left(\dot{m}_{k,j+\frac{1}{2}} - \left|\dot{m}_{k,j+\frac{1}{2}}\right|\right)\begin{Bmatrix}\alpha\\ \alpha u\\ \alpha H\end{Bmatrix}_{k,R} + \begin{Bmatrix}0\\ p_{j+\frac{1}{2}}\alpha_{j+\frac{1}{2}}\\ 0\end{Bmatrix}$$

  - Consistent application of forces and heat transfer
  - Removed "decoding" step
- Rigorous verification using frozen solid phase to emulate nozzle walls
  - Subsonic and supersonic flows
  - Match to isentropic properties
- Investigate effect in shock tube (no analytic solution)

Eulerian-Eulerian AUSM+up flux scheme has been extended to an Eulerian-Lagrangian formulation.

Key Results

- Quantified Eulerian-Lagrangian coupling error, Gaussian PB method
  - Calculates volume fraction at any point in the flow field
  - Reduces deterministic error
  - Provides sub-grid resolution
- Implemented EL flux scheme, AUSM+up
  - Balanced pressure flux for single phase
  - Consistently applied force and heat transfer
  - Frozen flow example matches isentropic solution
- Simulation matches experimental data well

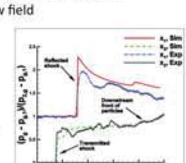

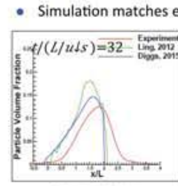

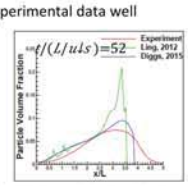

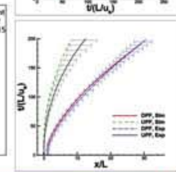

UF UNIVERSITY of FLORIDA

NNSA

CCMT

Center for Compressible Multiphase Turbulence

Shock & Contact Particle Interactions

Student: Christopher Neal
Advisor: Dr. S. Balachandar
Department: MAE, UF

- Goals
  - Advance Point-Particle Models
  - Multiple Particle Shock Interaction Simulations
  - Contact-Interface Simulations
- Simulation roadmap
  - This simulation work contributes data for the impinging shock & contact(density gradient) over single & arrays of particles to be used for advanced point-particle models.

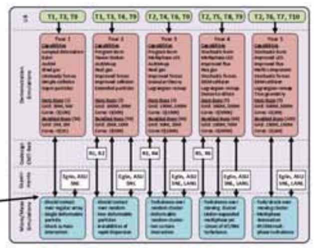

Simulation Roadmap

Why Use Point-Particle Models?

- Point-particle (PP) models approximate forces that particles in a flow feel under different flow conditions
- PP models reduce the need for resolution around particles
- The reduced computational footprint of simulations have
  - Millions of particles
  - Large spatial scales
- PP modeling work has focused on the force that an isolated particle in an incompressible or weakly (Ma~1.0) compressible flow experiences

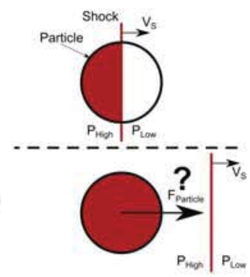

Random Particle Shock Results

- A randomly packed domain with 200 stationary particles with total volume fraction of 10% was subjected to an impinging shock with Mach number of 3.0
- The goal is to examine the force fluctuations that the particles feel
- A large coalesced bow shock forms on the leading edge of the particle pack

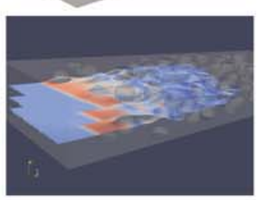

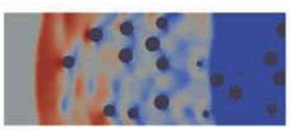

Random Particle Shock Results

- Drag coefficients for beds with volume fractions of 10, 15, 20, and 25%
- Particle shielding effects are evident in drag plots

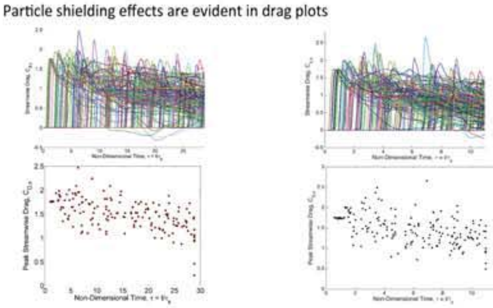

Random Particle Shock Results

- Flow variations within the particle bed are generated from neighbor reflections and flow nozzling between particles
- Particle bed interiors experience strong flow nozzling that produces regions of supersonic flow higher than the standard post-shock Mach number

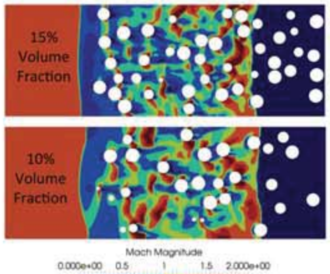

Year 3 Goals

- Expand simulation Mach number design space to include Mach numbers of 1.65 (experimental case conditions) and 1.22 (no nozzling to supersonic flow)
- Simulate same conditions with viscous effects introduced to examine the effects of vortex shedding on particle drag coefficients
- Study simulation using conditions similar to experiments to obtain metrics for comparing simulation results to experimentally measured quantities

UF UNIVERSITY of FLORIDA · NNSA

CCMT

Center for Compressible Multiphase Turbulence

RocSDT: Shock-Particle Interaction in Air

Student: Prashanth Sridharan
Advisor: Dr. S. Balachandar
Department: MAE, UF

- Goals
  - Investigate aluminum spherical particles under various shock loading conditions
  - Produce transient drag coefficient curves
  - Simulate Eglin experiments at the microscale
- Simulation roadmap
  - Develop transient force/drag histories for the Demonstration Problem

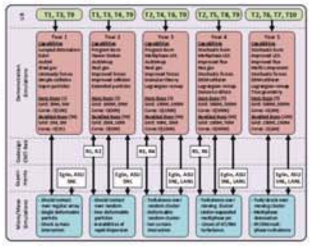

Simulation Roadmap

Motivation/Background

- **Purpose:** quantify momentum exchange of a particle under shock loading through the imparted transient drag coefficient curve, which can be used to create correlations, for point-particle force models, and kernels for larger scale simulations
- The present work focuses on early time behavior of shock-particle interaction, which is dominated by inviscid mechanisms
- The particle and medium are governed by

$$\frac{\partial \rho}{\partial t} + \nabla \cdot (\rho \vec{u}) = 0 \qquad p = (\gamma - 1)\rho e - \gamma P^{\infty}$$

$$\frac{\partial (\rho \vec{u})}{\partial t} + \nabla p + \nabla \cdot (\rho \vec{u}\vec{u}) = 0$$

$$\frac{\partial E}{\partial t} + \nabla \cdot ((E + p)\vec{u}) = 0$$

$$\frac{\partial \phi}{\partial t} + \vec{u} \cdot \nabla \phi = 0$$

Results – Single Particle Validation

- Grid resolved simulation is validated, with excellent agreement, with published experimental results
- Once validated, simulations are conducted at incident shock Mach numbers up to 10
  - The peak drag coefficient is found to decrease with increasing Mach number

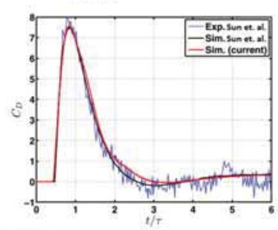

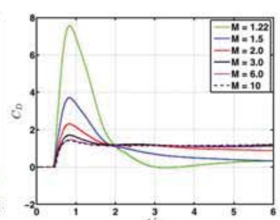

Results – Effect of Particle Spacing

- Shock-particle dynamics at various inter-particle spacing
  - Peak drag coefficient increase is influenced by the incident shock Mach number and inter-particle spacing
  - Particles' peak drag coefficient has a maximum
  - Peak drag ratio drops below one as inter-particle spacing goes to zero

Shock Mach number – 6.0

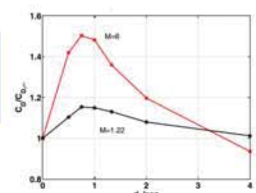

Results – Effect of Particle Deformation

- Goal: Study effect of particle deformation
- Example – Aluminum particle in Nitromethane

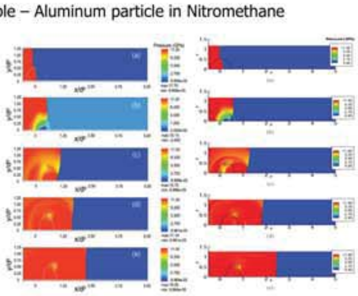

ALE3D RocSDT

Year 3 Goals

- Extend code to three-dimensions
- Parallelize code using MPI
- Simulate microscale experiments from Eglin
- Understand combined shock and material interface at high pressure on drag
- Develop point-particle force models to be used at the macroscale

UF UNIVERSITY of FLORIDA NNSA

CCMT

Center for Compressible Multiphase Turbulence

Modeling the Force Variation within Random Arrays of Spheres

Student: Georges Akiki
Advisor: Prof. S. Balachandar
Department: MAE, UF

- Goals
  - Quantifying the force variation within random arrays
  - Developing the next generation of point-particle force models that can reflect the force variation
- Simulation roadmap
  - Improved forces on particles at the meso and macroscale

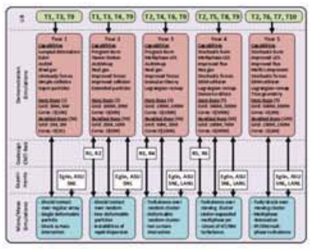

Simulation Roadmap

Motivation

- Perform fully-resolved DNS simulations of a pressure-driven flow past random arrays of spheres at different volume fraction $0.1 \le \phi \le 0.44$ and Reynolds number $2 \le Re \le 636$
- Quantifying the particle-to-particle force variation with respect to the array mean drag. This variation reflects the error introduced from using mean drag models.
- Developing a new model which returns a unique drag and lateral force for each sphere based on its unique position with respect to its neighborhood
- The new model would be the first to predict the drag variation and significantly reduce the error of classical mean drag models
- Lateral forces (set to zero in current mean models) could also be modeled and included in meso and macroscale simulations

Quantifying the Force Distribution (DNS data)

Case	*Mean Drag F_d*	*σ*	*σ/F_d*	*Skewness*	*Kurtosis*
$\phi = 0.1$, $Re = 170$	4.69	1.26	26.95%	-0.07	3.25
$\phi = 0.2$, $Re = 87$	2.48	0.61	24.71%	-0.17	2.94
$\phi = 0.4$, $Re = 20$	1.17	0.20	17.31%	0.22	2.81

Case	*Mean Lift*	*σ*	*σ/F_d*	*Skewness*	*Kurtosis*
$\phi = 0.1$, $Re = 170$	-8.4×10^{-4}	0.66	14.15%	0.21	3.84
$\phi = 0.2$, $Re = 87$	2.2×10^{-3}	0.33	13.19%	-0.02	3.60
$\phi = 0.4$, $Re = 20$	3.9×10^{-3}	0.18	15.16%	-0.02	3.59

- Significant drag and lateral force variation
- Skewness and Kurtosis reflect a Gaussian distribution of the forces
- Drag standard deviation/mean drag decreases with ϕ, no significant change with *Re*
- Lift standard deviation/mean drag does not significantly vary with ϕ nor *Re*

Pairwise Interaction Extended Point-Particle (PIEP) Model (1)

- Force on a single sphere in a steady non-uniform flow at finite *Re*:

$$F = 3\pi\mu d \boldsymbol{u}_{un}(1+0.15Re^{0.687}) + m_f(1+C_m)\frac{D\boldsymbol{u}_{un}}{Dt} + m_f C_{iL} \boldsymbol{u}_{un} \times \boldsymbol{\omega}_{un}$$

- Pairwise Interaction assumption:

$$\boldsymbol{u}_{un,i}(\boldsymbol{x}_i) \approx \boldsymbol{u}_{macro}(\boldsymbol{x}_i) + \sum_{j=1}^{N-1} \boldsymbol{u}'_{j\to i}(\boldsymbol{x}_i) \quad \text{(one neighbor at a time)}$$

- Evaluate force perturbation on a sphere (virtual) in a flow disturbed by the presence of one other sphere (solid)
- Systematically vary the location of virtual sphere to create a mapping of the force disturbance

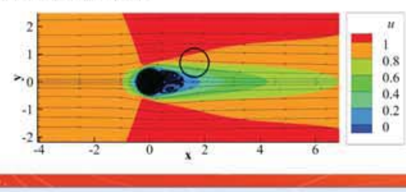

Pairwise Interaction Extended Point-Particle (PIEP) Model (2)

Velocity Perturbation Mappings. Similar mappings are created for F_{ll} and F_{RI}.

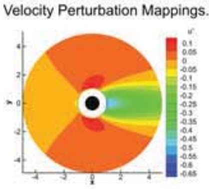

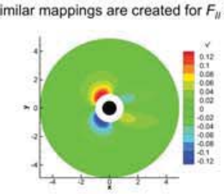

$$F_{QS,PI}(i) = \frac{3\pi}{Re}\left[(1,0) + \sum_{j=1}^{6}\overline{\left(\boldsymbol{u}'(\boldsymbol{x}_i - \boldsymbol{x}_j)\right)}^{S}_{map}\right]\left[1+0.15Re^{0.687}\right]$$

$$F_{ll,PI}(i) = \sum_{j=1}^{6} F_{ll,map}(\boldsymbol{x}_i - \boldsymbol{x}_j)$$

$$F_{RI,PI}(i) = \sum_{j=1}^{6} F_{RI,map}(\boldsymbol{x}_i - \boldsymbol{x}_j)$$

$$\boxed{F_{PIEP} = F_{QS,PI} + F_{ll,PI} + F_{RI,PI}}$$

Mean Force Model vs PIEP Model vs DNS (Results)

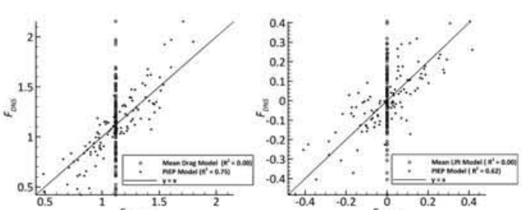

- Scatter plots of DNS forces on a single sphere in random arrays vs values predicted by models
- Frame 1 shows drag forces, and frame 2 shows lateral forces
- Comparable results obtained for different random array at $0.1 \le \phi \le 0.21$ and $16 \le Re \le 170$

UF UNIVERSITY of FLORIDA · NNSA

CCMT

Center for Compressible Multiphase Turbulence

Compressible Multiphase Turbulence Modeling

Student: Rahul Babu Koneru
Advisor: Dr. S. Balachandar
Department: MAE, UF

- Goals
  - Develop multiphase compressible LES model
  - Improved force modeling
  - Validation and integration into Rocflu and CMT-nek
- Simulation roadmap
  - Implement single phase LES and extend it to multiphase flows
  - Collaborate with microscale group to develop improved force models
  - Perform mesoscale simulations

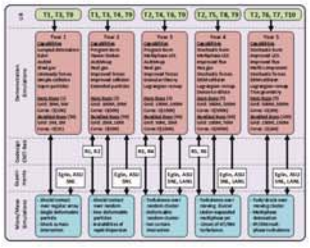

Simulation Roadmap

Governing Equations – LES Formulation

- Favre averaged single phase LES equations

$$\frac{\partial \bar{\rho}}{\partial t} + \frac{\partial \bar{\rho}\tilde{u}_i}{\partial x_i} = 0$$

Note: $\overline{(.)}$ = Filtered quantity, $\widetilde{(.)}$ = Favre-averaged quantity

$$\frac{\partial \bar{\rho}\tilde{u}_i}{\partial t} + \frac{\partial \bar{\rho}\tilde{u}_i\tilde{u}_j}{\partial x_j} + \frac{\partial \bar{p}}{\partial x_i} - \frac{\partial \check{\sigma}_{ij}}{\partial x_j} = -\frac{\partial \tau_{ij}}{\partial x_j} + \frac{\partial}{\partial x_j}[\overline{\sigma_{ij}} - \check{\sigma}_{ij}]$$

$$\frac{\partial \bar{\rho}\tilde{E}}{\partial t} + \frac{\partial (\bar{\rho}\tilde{E} + \bar{p})\tilde{u}_j}{\partial x_j} + \frac{\partial \check{q}_j}{\partial x_j} - \frac{\partial \check{\sigma}_{ij}\tilde{u}_j}{\partial x_j} = -\frac{\partial}{\partial x_j}[A_j + B_j - C_j + D_j]$$

Filtered pressure $\bar{p} = (\gamma - 1)\left[\bar{\rho}\tilde{E} - \frac{1}{2}\bar{\rho}\tilde{u}_i\tilde{u}_j - \frac{1}{2}\tau_{ii}\right]$

Favre averaged temperature $\tilde{T} = \frac{(\gamma-1)}{R}\left[\tilde{E} - \frac{1}{2}\tilde{u}_i\tilde{u}_j - \frac{1}{2\bar{\rho}}\tau_{ii}\right]$

Shear stress in terms of averaged quantities, $\check{\sigma}_{ij} = \mu(\tilde{T})\left[\left(\frac{\partial \tilde{u}_i}{\partial x_j} + \frac{\partial \tilde{u}_j}{\partial x_i} - \frac{2}{3}\frac{\partial \tilde{u}_k}{\partial x_k}\delta_{ij}\right)\right]$

Heat flux in terms of averaged quantities, $\check{q}_j = -k(\tilde{T})\frac{\partial \tilde{T}}{\partial \tilde{x}_j}$

Sub-grid scale terms,

$$A_j = \bar{\rho}\left[\widetilde{Eu_j} - \tilde{E}\tilde{u}_j\right], \quad B_j = \bar{p}\left[\overline{u_j} - \tilde{u}_j\right]$$

$$C_j = \overline{\sigma_{ij}u_j} - \check{\sigma}_{ij}\tilde{u}_j, \quad D_j = \overline{q_j} - \check{q}_j, \quad \tau_{ij} = \bar{\rho}\left[\widetilde{u_iu_j} - \tilde{u}_i\tilde{u}_j\right]$$

Mesoscale Simulations

- LES Modeling: Single phase open-ended shocktube [1]
- Force Modeling: Shock-particle curtain interaction

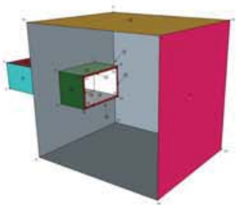

[1] *'Open-Ended Shock Tube Flows: Influence of Pressure Ratio and Diaphragm Position'*, A.Haselbacher, S. Balachandar and S. W. Keifer, AIAA Journal

Open-Ended Shocktube

- The Mach number and pressure behind the contact at the exit plane are plotted against time

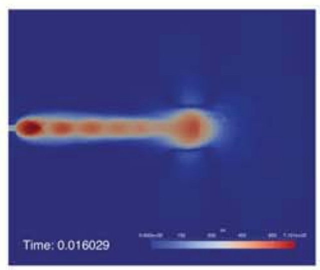

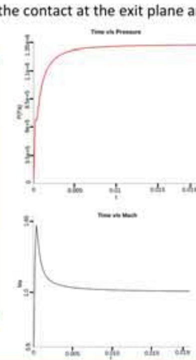

Shock-Particle Interaction

- Shown below is an image of shock interacting with a fixed bed of particles
- Eulerian-Lagrangian AUSM+up flux scheme is used in this simulation
- Shock Mach number = 3, No. of particles = 92960

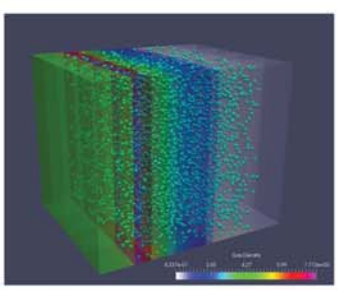

Summary & Year 3 Goals

- Summary
  - Simulations of single-phase jets with no turbulence model have been performed
  - Work is in progress to incorporate LES model into the code to study single-phase under-expanded jets
  - Developing new force models
- Year 3 Goals
  - Extend the single phase LES models to simulate multiphase flows
  - Develop both LES and force models to study flows with higher particle volume fractions

UF UNIVERSITY of FLORIDA · NNSA

CCMT

Center for Compressible Multiphase Turbulence

Particle Pressure Equation for Disperse Multiphase Flows

Dr. Subramanian Annamalai
Department: MAE, UF

- Goals
  - Analytical model to compute pressure variation in the dispersed phase when the carrier phase is subjected to complex flows
  - An equation for the pressure equilibration process analogous to particle equation of motion (Newton's second law)
- Simulation roadmap
  - Develop improved dynamic compaction equation/volume fraction evolution equation (T5) by generating pressure models for the dispersed phase

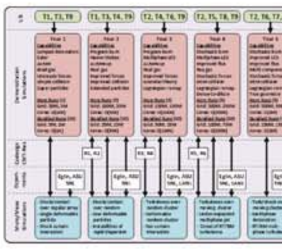

Simulation Roadmap

Motivation & Background

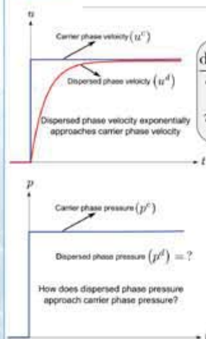

$$\frac{d\mathbf{u}^d}{dt} = \frac{\mathbf{u}^c - \mathbf{u}^d}{\tau_{pV}} \qquad \tau_{pV} = \frac{(2\tilde{\rho}+1)R_0^2}{9\nu^c\Phi_V}$$

$$\frac{dp^d}{dt} = ? \qquad \tau_{pP} = ?$$

The particle (dispersed phase) velocity response to changes in carrier phase velocity is well known and given by the particle equation of motion (e.g. Stokes drag law). The same hold true for temperature as well.

However an evolution equation governing particle pressure is unknown. Developing such a "pressure equilibration equation" is the goal of the current study.

This is achieved using acoustic analogy by solving the linearized compressible Navier-Stokes equations for both the dispersed and continuous phases.

Pressure Equilibration Equation

The volume-averaged particle phase pressure expressed purely in terms of "undisturbed" time-variation of the carrier phase properties is given as below

$$\overline{p^d}^V(t) = \overline{p_0^d}^V + \frac{R_0}{a_0^c}\int_{\tilde{\xi}=-\infty}^{\tilde{t}} K_p(\tilde{t}-\tilde{\xi})\left.\frac{d}{dt}\overline{p^c}^S\right|_{\tilde{t}=\tilde{\xi}} d\tilde{\xi} + R_0\int_{\tilde{\xi}=-\infty}^{\tilde{t}} K_w(\tilde{t}-\tilde{\xi})\left.\frac{d}{dt}\overline{(\rho u_r)^c}^S\right|_{\tilde{t}=\tilde{\xi}} d\tilde{\xi}$$

- $K_p(\tilde{t}-\tilde{\xi})$: Response to unit-step change in ambient pressure
- $K_w(\tilde{t}-\tilde{\xi})$: Response to unit-step change in ambient radial momentum
- $\overline{p_0^d}^V$: Initial particle pressure (volume averaged)
- $\frac{d}{dt}\overline{p^c}^S$: Time-varying ambient pressure (surface averaged)
- $\frac{d}{dt}\overline{(\rho u_r)^c}^S$: Time-varying ambient radial momentum (surface averaged)

R_0 : Mean particle radius, a_0^c : Ambient speed of sound

$K_p, K_w = f(\tilde{\rho}, \tilde{a})$ where $\tilde{\rho}$: density ratio, $\tilde{a}$: Speed of sound ratio

Kernel (K_p, K_w) & undisturbed flow properties

A normal shock (Ma = 1.11) passing over an aluminum sphere in nitromethane

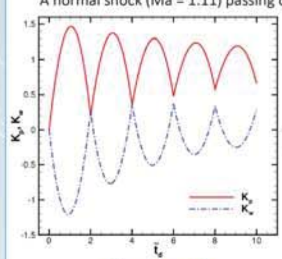

$Z = \tilde{\rho}\tilde{a} \approx 10$

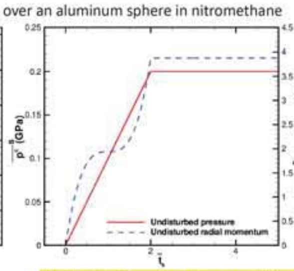

Undisturbed carrier phase quantities

- Oscillations represent acoustic waves traveling back and forth inside the particle
- Directly translates to oscillation in particle pressure

Pressure Evolution: Shock Ma = 1.11

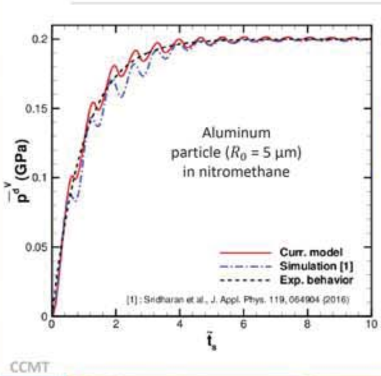

Exp. behavior (black-dash line) analogous to particle equation of motion:

$$\frac{d\overline{p^d}^V}{dt} = \frac{p^c_{\text{final}} - \overline{p^d}^V}{\tau_{pP}}$$

$\tau_{pP} = R_0/u_s$ is the particle time-scale

Similar agreements also observed for higher Mach numbers and particles with larger radii.

Summary & Year 3 Goals

- Summary
  - Developed a "pressure equilibration" equation to compute time-dependent pressure in the dispersed phase subjected to any complex inhomogeneous carrier phase variation
  - Expressed the particle pressure as comprising of two parts (i) kernel, that accounts for the temporal changes and (ii) surface average carrier phase quantities that account for spatial variation
  - Applied the model to predict pressure inside an aluminum sphere (5 μm radius) as a normal shock (Ma=1.11) wave sweeps past the particle; and found good agreement with the numerical results
- Year 3 Goals
  - Empirically extend the present analysis to account for finite Re and Ma flows (carrier phase)
  - Develop a surrogate model for the kernels (K_p, K_w), which is a function of the first maxima, frequency, density and speed of sound ratios

UF UNIVERSITY of FLORIDA · NNSA

CCMT

Center for Compressible Multiphase Turbulence

Microscale – Shock Particle Interaction

Student: Yash Mehta
Advisor: Dr. S. Balachandar
Department: MAE, UF

- Goals
  - Fully resolved DNS of shock particle interaction
  - Developing models for predicting force history on particles
- Simulation roadmap
  - Shock Particle Interaction with structured array and randomly distributed particles
  - Integration of force models in Meso-Macro scale simulations

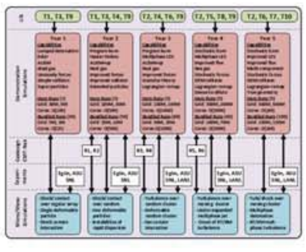

Simulation Roadmap

Motivation

- There is a need for understanding the interaction of high pressure - high temperature flow with the particles
- Fully resolved Direct Numerical Simulations are used to obtain force history on particles and understanding the underlying physical phenomena during shock particle interaction
- Results from DNS are used to develop models for predicting the motion of particles in complex flows

Shock Interaction with FCC Array of Particles

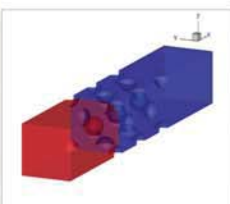

	$\varphi = 10\%$	$\varphi = 20\%$	$\varphi = 30\%$	$\varphi = 40\%$
$M_s = 1.5$	RUN1	RUN5	RUN9	RUN13
$M_s = 2.0$	RUN2	RUN6	RUN10	RUN14
$M_s = 3.0$	RUN3	RUN7	RUN11	RUN15
$M_s = 6.0$	RUN4	RUN8	RUN12	RUN16

- Matrix of simulations were performed to understand the effect of shock Mach number and volume fraction
- Simulation setup had 2 units cells of particles arranged in face centered cubic (FCC) arrangement

Shock Interaction with FCC Array of Particles

$\varphi = 10\%$
$M_s = 1.5$

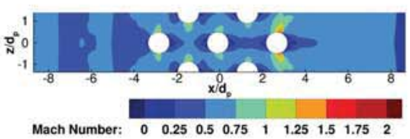

$\varphi = 40\%$
$M_s = 6.0$

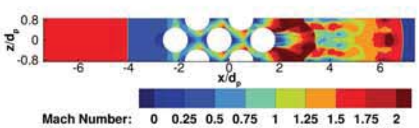

FCC - Effect of Mach number; $\varphi = 10\%$

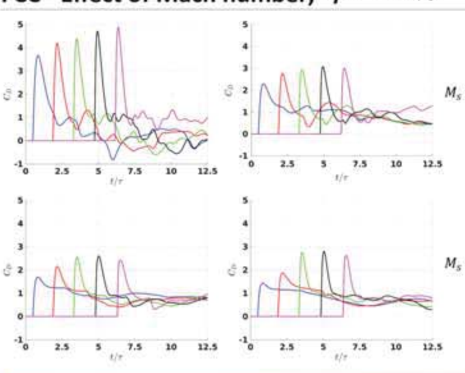

FCC - Effect of Volume-fraction; $M_s = 1.5$

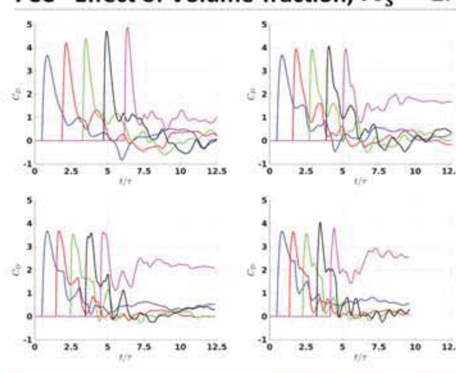

UF UNIVERSITY of FLORIDA · NNSA

CCMT

Center for Compressible Multiphase Turbulence

Performance, Energy and Thermal Research

Dr. Tania Banerjee

Department: CISE, UF

- Goals
  - Performance, energy and thermal optimization framework applied to CMT-nek on a variety of platforms
  - Provide performance data to Exascale team for modeling
  - Development and validation of a proxy app for CMT-nek
  - Load balancing algorithms for particulate applications applied to CMT-nek
- Simulation roadmap
  - Our research roadmap is closely tied with CMT-nek development

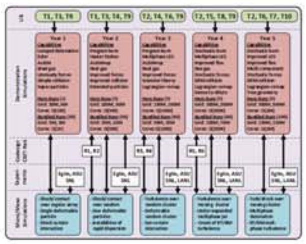

Simulation Roadmap

Motivation: Performance/Energy Optimization

- CPU performance improvement of derivative computation kernel

Platforms	CMT-nek time (secs)	Exhaustive Autotuning			GA based Autotuning			
		Time	Search Space	%Less	Time	Search Space	% Less	%Diff
IBM BG/Q	5.57	2.54	97716	54.3	2.58	1124	53.7	1.1
AMD Opteron	1.81	1.02	97716	43.6	1.06	1283	41.4	3.9
AMD Fusion	1.36	0.95	32652	30	0.95	485	30	0.0

- CPU energy consumption of derivative computation kernel

Platforms	CMT-nek energy (Joules)	Exhaustive Autotuning			GA based Autotuning			
		Energy	Search Space	%less	Energy	Search Space	% Less	%Diff
IBM BG/Q	292.1	131.7	97716	54.9	135	1124	53.7	2.5
AMD Fusion	17.6	11.98	32652	32	12.11	485	31	1.1

- GPU performance: Mohamed Gadou has the details

Energy/Performance Tradeoff

- Case study: derivative computation kernel

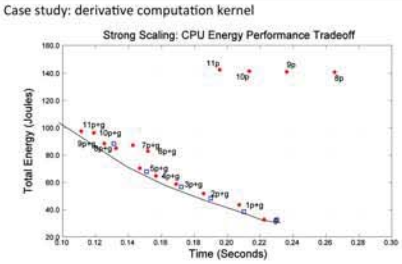

- Circles represent performance optimal load balancing: CPU and GPU finish processing at about the same time
- Squares represent energy optimal load balancing: Given a deadline, the GPU should process most of the load with the remaining load being processed by the CPU

CMT-bone

- Identified workflow, key data structures and kernels of CMT-nek

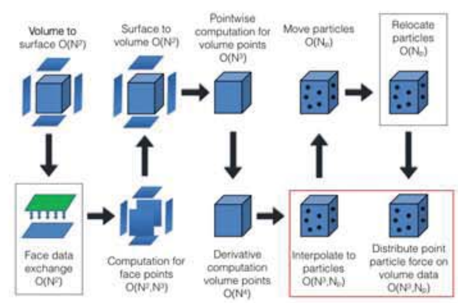

CMT-bone Validation in Collaboration w/LLNL

- Used VERITAS on performance results from Intel Xeon with scaling of cores
  - Performance bottlenecks common in parent and proxy app are identified
- Common bottlenecks in communication stage

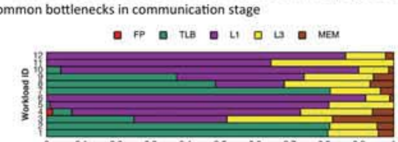

- Common bottlenecks in point computation stage

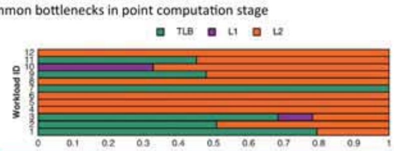

CMT-bone Validation in Collaboration w/LLNL

- Common bottlenecks in the computation kernel

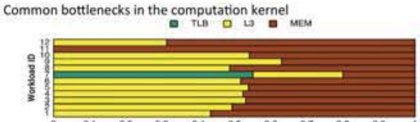

- Common bottlenecks in the particles processing kernel

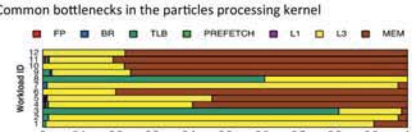

- Overall assessment: performance loss with scaling in CMT-nek is caused by cache misses and access to high-latency node memory
- CMT-bone captures these performance characteristics well

UF UNIVERSITY of FLORIDA

NNSA

CCMT

Center for Compressible Multiphase Turbulence

Hybrid Performance of CMT-bone

Student: Mohamed Gadou
Advisor: Dr. Sanjay Ranka
Department: CISE, UF

- Goals
  - Implementation of CMT-bone on a hybrid processor with GPU accelerator
  - Performance optimization of various key computation kernels
  - Load balance computation between CPU and GPU
- Simulation roadmap
  - Our research roadmap is closely tied with CMT-nek development

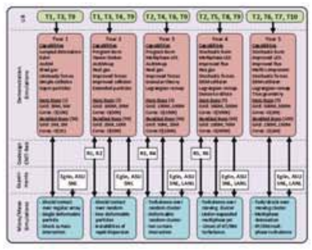

Simulation Roadmap

Motivation

- Hardware Software co-optimization by adding hardware parameters like cache line and associativity
- Hybrid Implementation of cmtbone to benefit from GPU computation power
- Master-slave
- CPU sends function and operator matrices to GPU, GPU computes derivatives. Reduce communication.

Host:
AMD Opteron 6274
16 cores
2.2 GHz clock frequency

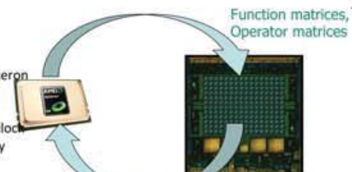

Tesla K20:
13 Processors
192 Cores
48k shared memory
64k registers
1170 GFLOP/s Peak
706MHz clock frequency

Hardware Software Co-optimization

- Hardware parameters
  - L1 cache size – 2K, 4K, 8K
  - L1 line size – 64, 128, 256
  - L1 associativity – 2, 4, 8

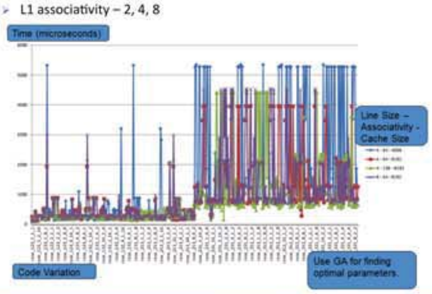

Hybrid Performance for Derivative Kernel

- With a single CPU core, GPU processes about 4-9 times more load
- Derivative computation involves matrix multiplication and has a complexity of O(N4)

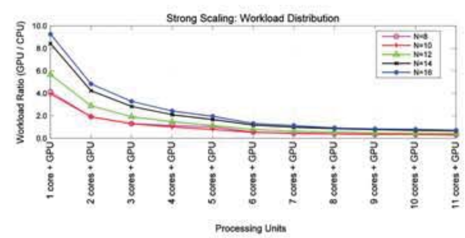

GPU Performance – per kernel – On Titan

- Per kernel performance on GPU relative to CPU – 8000 elements

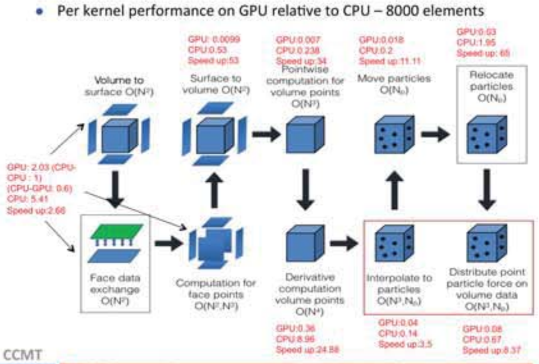

GPU Performance – Overall – On Titan

- Overall Performance

Number of elements	1 CPU (with comm)	1 CPU (excluding comm)	1 GPU (with comm)	1 GPU (excluding comm)	Speed-up (with comm)	Speed-up (excluding comm)
4096	8.24 seconds	7.7 seconds	1.4 seconds	0.86 seconds	5.88	8.95
8000	17.86 seconds	16.86 seconds	2.83 seconds	1.83 seconds	6.31	9.21

- More Enhancements
  - Reduce CPU-GPU communication more

UF UNIVERSITY of FLORIDA

NNSA

CCMT

Center for Compressible Multiphase Turbulence

SST-based BE Simulation Platform

Students: Parth Shah, Nalini Kumar, Dylan Rudolph
Advisor: Prof. Herman Lam, Prof. Alan George, Prof. Greg Stitt
Department: ECE, UF

- Goals - Adopt an existing simulation framework for Behavioral Emulation (BE) to:
  - Scale BE simulations to Exascale number of components
  - Increase developer productivity by using existing and well-supported tools & methods
- Simulation roadmap
  - BE-SST integration will enable CCMT to scale BE simulations to millions of components which is necessary for simulating Exascale systems
  - Assist in early algorithm design space exploration at different stages in the CCMT simulation roadmap

CCMT Simulation Roadmap

Motivation for BE-SST Integration

SST (Structural Simulation Toolkit) @ SNL

- Provides a simulation framework suitable for coarse-grained, parallel simulations – *valuable for scaling simulations*
- Supported by a team of developers and vendors that contribute to model libraries that can be leveraged for BE
- Provides much *flexibility in component design* – useful for designing Behavioral Emulation Objects (BEOs) while still using event-handling capabilities provided by SST

SST Capabilities		*BE Influences*		*Desired Capabilities*
• Framework (core) • Network Models • Component Models	+	• Software Definitions • Probabilistic Simulation • Abstract Network Definitions • Abstract Hardware Definitions	=	• Framework (Sim. Environment) • Software Definitions • Probabilistic Simulation • Abstract Network Models • Abstract Component Models

Overview: SST and BE-SST

- **SST Core**
  - SST Core is framework that handles interactions between SST Components
  - Includes interfaces, definitions, and utilities for building simulation models
- **SST Elements**
  - SST Elements are simulation models built using SST Cores
- **SST simulations**
  - SST Components are connected via SST Links
  - Interactions / communication occur via Events over Links
  - Event Handlers to handle events
  - Enable parallel simulations

Mapping BE onto SST design constructs

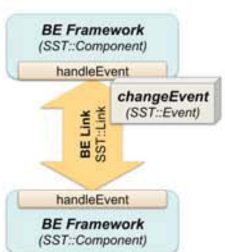

BE-SST Simulation Workflow

- Software definitions and system definitions are independent of the simulation platform and compiled outside the BE-SST Simulator
- These definitions are translated into AppBEO & ArchBEO which are translated into BE-SST Components & simulated

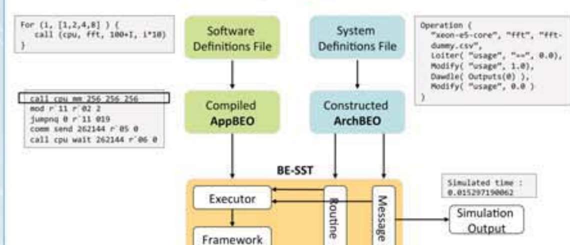

Modules in BE-SST

BE-SST

Simulator: creates network configuration; maintains a list of AppBEOs

Framework	Main SST component that drives the simulation

Processes: generate events responsible for changing simulation state

Executor	Executes AppBEO & generate events for creating child processes
Routine	Based on input event type, returns an event that may/may not change simulation state
Message	Generates events that may change state of components nodes in communication path

Events defined in simulation processes:

- changeEvent, conditionEvent, timeoutEvent, autoprocessEvent, subprocessEvent, terminateEvent,

Summary

Conclusions & Future Work

- Implementation of BE functionality on SST *in progress*
- Exploring optimizations & how best exploit SST capabilities
  - Parallelism
  - Scalability
- Exploring alternative architectures (e.g. possibility of having different components for different ArchBEO types)
- Exploring use of (leveraging) existing SST elements
- Apply the lessons learned for v1 BE-SST prototype due at end of cycle 2 (Dec 2016)

UF UNIVERSITY of FLORIDA

CCMT

Center for Compressible Multiphase Turbulence

FPGA Pipelined Simulations for CMT-nek

Students: Carlo Pascoe, Kasim Alli

Advisors: Dr. Stitt, Dr. Lam

- Design-space exploration (DSE) critical in optimization of CMT-nek for potential Exascale architectures
  - CMT-nek has huge design space (DS)
  - BE is a potential solution, but is it enough?
  - Complement and accelerate BE approach via FPGA acceleration
  - Propose pipelined data flow simulations as useful technique for rapid exploration under certain circumstances

Simulation Roadmap

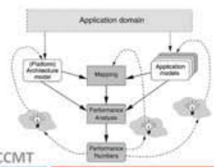

- Goal: pipeline simulations to explore a different design option every cycle
  - After some initial latency, quickly explore large number of different configurations – fast DSE
- Ideal for an FPGA
  - Pipeline is bounded by resources rather than I/O
  - Multiple FPGAs can be used to explore a vast input space – almost embarrassingly parallel
  - **Up to eight orders-of-magnitude faster DSE**

CCMT 1

Use Cases for Pipelined Simulation

Massive CMT-nek DS — Potential for millions of options per architecture

1) Entry point for pipelined DSE: limited in precision and data quantity logged, but capable of processing potentially thousands of sims/second.

Pruned DS — Only promising design candidates progress

2) Entry point for SW BE : Explore potential (pruned or complete) candidates with full analysis capabilities. Order of mins per simulation, but potentially more accurate.

Final Predictions — Desire to build confidence in simulation predictions

3) Entry point for pipelined Monte Carlo simulations: Combine desire to rerun single simulation thousands of times with ability to process thousands of simulations per second!

Optimal Design Configurations

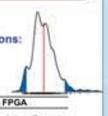

Pipelined Simulation Concept:

- Map threaded AppBEO to data flow graph
- Per thread, each AppBEO instruct and its operand/output dependencies mapped to a DFG vertex and edges respectively
- DFG maps directly to pipelined circuit
  - Each vertex instantiates dedicated instruct HW
  - Each edge instantiates a pipeline reg between src/dst vertices (i.e., src/dst instructions)
- Because each instruction from **entire** Sim is mapped to independent HW (no resource sharing), each vertex is able to start next sim 1 cycle after current sim

Pipelined MC simulation of CMT-nek-abstract on Stratix V GSMD8 FPGA

Architecture Configuration	Latency to first simulation output	FPGA Clk frequency	% Logic utilization (in ALMs)	Simulations/Second
cab-8	18 cycles	290 MHz	2%	**290,000,000**
cab-64	21 cycles	265 MHz	17%	**265,000,000**
cab-216	23 cycles	240 MHz	57%	**240,000,000**

CCMT 2

Pipelined Simulations : Approach

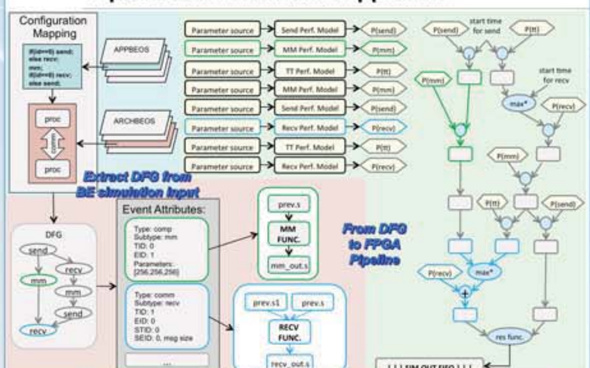

CCMT 3

Key Research Challenges

- Given infinite resources, DFG mapping for arbitrary BE simulation is straight forward, however practical limitations (e.g, resources, synchronization) necessitate more effective mappings
  - Scale limited to single FPGA without additional design effort
  - Event synchronization drastically increases resource usage due to potentially long delay register chain insertion
  - Quantity of raw data processed/generated intra-FPGA on a single clock cycle is massive–must be more selective of data logged per simulation
  - Static pipeline limits DSE sweeps to parameter subset that does not effect application control flow
- Many potential optimizations/solutions (current & future work)
  - e.g., event merging, tree-height reduction, partial loop "re-rolling", dynamic range analysis, shared performance models, targeted event monitoring instead of exhaustive, FPGA overlays or intermediate fabrics
  - Many optimizations complement one another, producing synergistic performance gains when applied in the correct sequence
- Challenge becomes how to apply various optimizations to automatically generate "best" circuit implementation for generic BE DFG
  - DSE of DFG mapping to aid DSE of CMT-nek

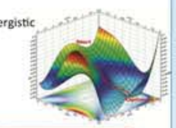

CCMT 4

Conclusions and Future Work

- Conclusions
  - Prospect of exploring massive CMT design space motivates evaluation of faster simulation approach
  - We identified pipelined simulations as promising alternative and evaluated its utility for massively parallel simulation of BE on FPGAs
    - E.g., created test circuit capable of performing MC simulation of CMT-bone case study at 240 Mega-sims/second compared to SW simulator at 4 sims/second
  - We identified key research challenges associated with practical application of the pipelined simulation approach and proposed potential solutions
- Future work:
  - Increase the scale of our FPGA-accelerated simulations prompting immediate exploration of efficient resource sharing and extension of single DFG pipelines to multiple FPGAs

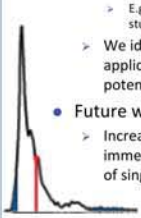

CCMT 5

Example DFG Pipeline Optimizations

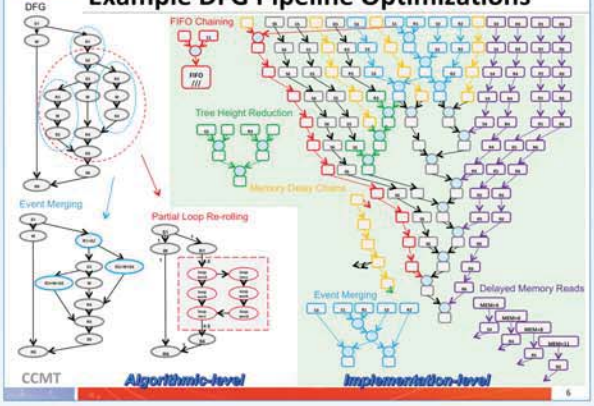

CCMT 6

CCMT

Center for Compressible Multiphase Turbulence

Scaling Behavioral Emulation (BE) Methodology for System Simulation

Student: Dylan Rudolph, Nalini Kumar
Advisor: Prof. Herman Lam, Prof. Greg Stitt, Prof. Alan George
Department: ECE, UF

- Goals
  - Apply BE methodology, demonstrated for device simulations during AST review '15, to node- and system-level simulations
  - Design & validate simulation models of existing architectures; lay foundation for prediction of notional systems
- CCMT Simulation roadmap
  - Enable early algorithm design space exploration (DSE) to aid and assist CMT-nek code developers at different stages in simulation roadmap

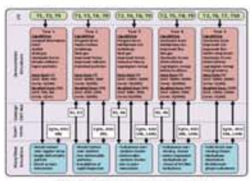

CCMT Simulation Roadmap

Motivation and Guiding Principles of BE

- Allow performance analysis at different levels of system organization (device, node, rack, machine) – *Multi-scale simulation*
- Allow use of performance models agnostic of how they were developed (testbed experiments, fine-grained simulation, analytical models, etc.) – *Component-based simulation*
- Allow arch DSE by providing ability to build notional archs by plugging different components in simulation – *Component-based simulation*
- Allow fast algorithm DSE by simulation from high-level scripts, and not requiring working code – *Coarse-grained simulation*
- Allow reasonably accurate performance analysis within a reasonable time – *Coarse-Grained Simulation*
- Finally, ensure simulation approach is portable to any PDES framework

CMT-nek code developers will be able to use BE simulation capabilities to analyze performance on future systems, understand potential bottlenecks, and revise code development plan accordingly

Application Modeling

Real Application (snippet from CMT-bone-BE)

Instrumentation and Model Generation

- Insert timing functionality into important parts of application
- Benchmark it over parameter space
- Convert these into BE models

App-BEO (snippet from CMT-bone-BE)

Simulation and Analysis

- Run App-BEO through simulator, along with an Arch-BEO
- Obtain runtime information (possibly probabilistic) for this App/Arch pair
- Sweep over different parameters of interest (elementSize, elementsPerProcess)

Architecture Modeling

- Identify important portions of machine from modeling perspective
- Identify component hierarchy and symmetries
- Apply any reasonable simplifying assumptions (example: multi-level tree of switches in Cab@LLNL can be modeled as a single level of switch)

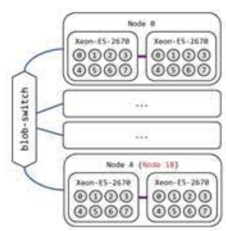

Cab Model

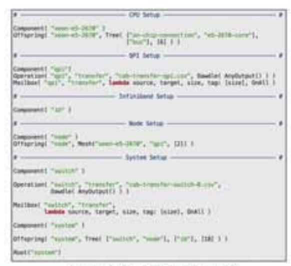

Arch-BEO (snippet from Cab model)

Simulation Output and Results

Currently, BE simulations output the following two metrics:

- Execution Time:
  - Deterministic or probabilistic (right) execution time of a given App/Arch pair
  - Accurate simulations possible even with limited information or large systems
- Hardware Utilization:
  - Determine which components are under-utilized for a given candidate algorithm
  - Determine load-over-time on, say, network components or accelerators

Simulated and real execution time (per CMT-nek timestep)

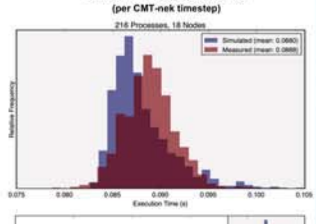

Setup:

- CAB @ LLNL
- 216 processes (6x6x6 Cartesian grid)
- 6 of 8 cores used in each processor
- Histogram of 1000 measured & simulated runs
- (128-512) samples per model

Summary

Conclusions

- Extended BE framework for modeling nodes and systems
- Added capability to perform Monte-Carlo based BE simulations
- Reasonable accuracy for small system sizes

Future Work

- Energy considerations: determine, on a per-component basis, which things are using the most energy
- Performance & energy considerations: determine which candidate algorithms and architectures are most efficient
- Reliability considerations: determine which algorithms and architectures perform well under prescribed failure conditions

UF UNIVERSITY of FLORIDA · NNSA